A STUDY ON THE EFFECTS OF GAMMA RADIATION ON THE PROPERTIES OF POLYCARBONATE

A THESIS SUBMITTED TO
THE GRADUATE SCHOOL OF NATURAL AND APPLIED SCIENCES
OF
MIDDLE EAST TECHNICAL UNIVERSITY

BY

KERİM GÖKHAN KİNALIR

IN PARTIAL FULFILLMENT OF THE REQUIREMENTS
FOR
THE DEGREE OF MASTER OF SCIENCE
IN
POLYMER SCIENCE AND TECHNOLOGY

FEBRUARY 2011

Approval of the thesis:

A STUDY ON THE EFFECTS OF GAMMA RADIATION ON THE PROPERTIES OF POLYCARBONATE

submitted by **KERİM GÖKHAN KİNALIR** in partial fulfillment of the requirements for the degree of **Master of Science in Polymer Science and Technology Department, Middle East Technical University** by,

Prof. Dr. Canan Özgen _____
Dean, Graduate School of **Natural and Applied Sciences**

Prof. Dr. Necati Özkan _____
Head of Department, **Polymer Science and Technology**

Prof. Dr. Ali Usanmaz _____
Supervisor, **Polymer Science and Tech. Dept., METU**

Prof. Dr. Cevdet Kaynak _____
Co-Supervisor, **Polymer Science and Tech. Dept., METU**

Examining Committee Members:

Prof. Dr. Zuhal Küçükyavuz _____
Polymer Science and Technology Dept., METU

Prof. Dr. Ali Usanmaz _____
Polymer Science and Technology Dept., METU

Prof. Dr. Ahmet M. Önal _____
Polymer Science and Technology Dept., METU

Prof. Dr. Cevdet Kaynak _____
Polymer Science and Technology Dept., METU

Assoc. Prof. Dr. Tonguç Özdemir _____
Engineer, TAEK

Date: 10 / 02 / 2011

I hereby declare that all information in this document has been obtained and presented in accordance with academic rules and ethical conduct. I also declare that, as required by these rules and conduct, I have fully cited and referenced all material and results that are not original to this work.

Name, Last name : Kerim Gökhan Kinalır

Signature :

ABSTRACT

A STUDY ON THE EFFECTS OF GAMMA RADIATION ON THE PROPERTIES OF POLYCARBONATE

Kinalır, Kerim Gökhan

M.Sc., Department of Polymer Science and Technology

Supervisor : Prof. Dr. Ali Usanmaz

Co-Supervisor : Prof. Dr. Cevdet Kaynak

February 2011, 71 pages

This thesis aims to investigate the effects of gamma radiation on the properties of polycarbonate, an engineering thermoplastic which has a wide range of applications. A commercial grade polycarbonate resin, after being shaped into the required specimen forms by injection molding, was irradiated with different doses up to 180 kGy. Tensile strength was found to decrease with increasing dose. The lowest values of tensile modulus, flexural modulus and flexural strength were obtained at 96 kGy, which is also the dose at which molecular weight values showed a minimum. No remarkable changes in Shore D hardness values and NMR spectra were observed. The ATR-FTIR spectra showed that irradiation was effective on carbonyl groups in the structure. The glass transition temperatures of the specimens irradiated up to the maximum dose were lower than those of the non-irradiated specimens. The onset of weight loss at lower temperatures and steeper weight loss behavior in the TGA curves indicated decreasing thermal stability of the polymer with increasing dose.

Keywords: Gamma irradiation, polycarbonate

ÖZ

GAMA RADYASYONUNUN POLİKARBONATIN ÖZELLİKLERİNE ETKİSİ ÜZERİNE BİR ÇALIŞMA

Kinalır, Kerim Gökhan
Yüksek Lisans, Polimer Bilimi ve Teknolojisi Bölümü
Tez Yöneticisi : Prof. Dr. Ali Usanmaz
Ortak Tez Yöneticisi : Prof. Dr. Cevdet Kaynak

Şubat 2011, 71 sayfa

Bu tezde, gama radyasyonunun yaygın uygulama alanına sahip bir mühendislik termoplastiği olan polikarbonatın özelliklerine etkisinin incelenmesi amaçlanmıştır. Granül halde ticari kalite bir polikarbonat, enjeksiyon kalıplama ile gereken numune şekillerine getirildikten sonra 180 kGy'e kadar değişik dozlarda ışınlanmıştır. Çekme dayancının artan dozla azaldığı görülmüştür. Çekme modülü, eğme modülü ve eğme dayancının en düşük değerleri; aynı zamanda moleküler ağırlık değerlerinin de minimum olduğu 96 kGy'de elde edilmiştir. Shore D sertlik değerleri ve NMR spektrumlarında belirgin değişiklikler gözlenmemiştir. ATR-FTIR spektrumları, ışınlamanın karbonil grupları üzerinde etkili olduğunu göstermiştir. En yüksek dozda ışınlanan numunelerin camsı geçiş sıcaklıkları, ışınlama görmemiş numunelerinkinden daha düşük çıkmıştır. TGA eğrilerinde ağırlık kaybının daha düşük sıcaklıklarda başlaması ve daha hızlı ağırlık kayıp davranışı, artan dozla polimerin termal kararlılığının azaldığını göstermiştir.

Anahtar Kelimeler: Gama ışınlama, polikarbonat

To everybody who have loved and supported me in my life

ACKNOWLEDGMENTS

I am grateful to my supervisor Prof. Dr. Ali Usanmaz and my co-supervisor Prof. Dr. Cevdet Kaynak for their guidance, support and advice throughout this study.

I wish to thank to all faculty members of the Department of Polymer Science and Technology whom I had the privilege of being their student, especially to Prof. Dr. Leyla Aras, for her kind support in every stage of my graduate study as well as the knowledge and insight she introduced me on polymers.

During the experimental work I carried out in this thesis I was helped by many nice, hardworking and smart research assistants. Among them Ms. Elif Vargün (now a faculty member at Muğla University), Mr. Ali Işıtman and Mr. Mehmet Doğan deserve special thanks. I strongly believe that a bright career awaits them in the future. In this context, thanks also go to Ms. Tuğba Efe. It was very kind of Prof. Dr. Göknur Bayram and Ms. Sibel Dönmez to help me carry out injection molding trials at the Department of Chemical Engineering. I am also indebted to Ms. Sevim Ulupınar for the DSC and DMA work, and also to the specialists at NMR laboratories.

Thanks to the staff at Turkish Atomic Energy Authority (TAEK), especially to Assoc. Prof. Dr. Serdar Karadeniz and Dr. Hande Karadeniz, for their contribution at the irradiation stage of this study. I would also like to thank to Assoc. Prof. Dr. Tonguç Özdemir for his interest in my study and valuable suggestions.

My special thanks are to Ms. Ayşegül Gediközer Elmacı and Ms. Neslihan Gökçe for their friendship, help and kindness. They have the biggest share in what makes the years of my graduate study in this department a pleasant memory.

Finally, I am deeply indebted to my parents for their love, encouragement and support not only during this study but throughout all my life.

TABLE OF CONTENTS

ABSTRACT……iv
ÖZ……v
ACKNOWLEDGMENTS……vii
TABLE OF CONTENTS……viii
LIST OF TABLES……x
LIST OF FIGURES……xi
CHAPTERS
1. INTRODUCTION……1
1.1 Polycarbonate……1
1.2 Ionizing Radiation and Its Interaction with Matter……4
1.3 Interaction of Ionizing Radiation with Polymers……6
1.4 Effects of Ionizing Radiation on Polycarbonate……10
1.5 The Aim of This Study……15
2. EXPERIMENTAL PROCEDURE……16
2.1 Material……16
2.2 Shaping of the Specimens……16
2.3 Irradiation of the Specimens……18
2.4 Mechanical Tests……18
2.4.1 Tensile Tests……18
2.4.2 Bending Tests……19
2.4.3 Hardness Tests……21
2.5 Molecular Weight Determinations……22
2.5.1 Dilute Solution Viscometry……22
2.5.2 Gel Permeation Chromatography……24
2.6 Spectroscopic Analyses……25
2.6.1 Infrared Spectroscopy……25
2.6.2 Nuclear Magnetic Resonance Spectroscopy……25
2.7 Thermal Analyses……26
2.7.1 Differential Scanning Calorimetry……26

2.7.2 Dynamic Mechanical Analysis……..……27
2.7.3 Thermogravimetric Analysis……..……28
3. RESULTS AND DISCUSSION……..……..……..……..……..……..……..……...30
3.1 Discoloration…..……..……..……..……..……..……..……..……..……30
3.2 Effects on the Mechanical Properties……31
3.2.1 Tensile Tests……..……31
3.2.2 Bending Tests……35
3.2.3 Hardness Tests……..……39
3.3 Effects on the Molecular Weight……..……40
3.3.1 Dilute Solution Viscometry……..……..40
3.3.2 Gel Permeation Chromatography……..……46
3.4 Effects on the Molecular Structure……..……48
3.4.1 Infrared Spectroscopy……48
3.4.2 Nuclear Magnetic Resonance Spectroscopy……..……52
3.5 Effects on the Thermal Behavior……56
3.5.1 Differential Scanning Calorimetry.....56
3.5.2 Dynamic Mechanical Analysis.....59
3.5.3 Thermogravimetric Analysis.....63
4. CONCLUSIONS.....66
REFERENCES.....68

LIST OF TABLES

TABLES

Table 3.1 Tensile modulus values of the test specimens……..…….…….33
Table 3.2 Tensile strength values of the test specimens……..……33
Table 3.3 Flexural modulus values of the test specimens……...……37
Table 3.4 Flexural strength values of the test specimens……..…38
Table 3.5 Shore D hardness values of the specimens……..……40
Table 3.6 Viscosity parameters of solutions of specimens at each irradiation dose……..……..41
Table 3.7 Intrinsic viscosities of solutions and the corresponding molecular weights of specimens……..……45
Table 3.8 Molecular weights of the three groups of specimens determined by GPC……...…….46
Table 3.9 Absorbance intensities at 1769 cm^{-1}, 767 cm^{-1} and oxidation indices at each dose……..52
Table 3.10 T_g values obtained from DSC curves of the specimens……58
Table 3.11 T_g of the specimens as tanδ peaks…….……...…...……..…….62

LIST OF FIGURES

FIGURES

Figure 1.1 Synthesis reactions of polycarbonate: (a) interface process, and (b) transesterification reaction [4]…….....……..……...…2
Figure 1.2 Picture showing various items made from polycarbonate.....3
Figure 2.1 Granules of polycarbonate used in this study…….……..…16
Figure 2.2 Injection molding machine used for shaping of the specimens.....17
Figure 2.3 (a) Dog bone, and (b) bar-shaped specimen.……17
Figure 2.4 Specimen gripping and supporting during (a) tensile, and (b) bending tests……20
Figure 2.5 Shore D durometer used in hardness measurements…….……22
Figure 3.1 Color change observed after irradiation doses of (a) 0, (b) 20, (c) 44, (d) 96, (e) 136, and (f) 180 kGy.....…30
Figure 3.2 Representative tensile stress-strain curves of the specimens irradiated up to (a) 0, (b) 20, (c) 44, (d) 96, (e) 136, and (f) 180 kGy……31
Figure 3.3 Effect of irradiation dose on tensile modulus…….……34
Figure 3.4 Effect of irradiation dose on tensile strength…….……34
Figure 3.5 Representative flexural stress-strain curves of the specimens irradiated up to (a) 0, (b) 20, (c) 44, (d) 96, (e) 136, and (f) 180 kGy……..…35
Figure 3.6 Effect of irradiation dose on the flexural modulus…….38
Figure 3.7 Effect of irradiation dose on the flexural strength……..39
Figure 3.8 Effect of irradiation dose on the Shore D hardness……40
Figure 3.9 Inherent viscosity versus concentration plots of the solutions of the specimens with irradiation doses of (a) 0, (b) 20, (c) 44, (d) 96, (e) 136, and (f) 180 kGy…….42
Figure 3.10 Effect of irradiation dose on the M_v the specimens…….....…….45
Figure 3.11 Effect of irradiation dose on the (a) M_n, (b) M_w, and (c) M_z of the three groups of specimens…….…..46
Figure 3.12 ATR-FTIR spectra of the specimens irradiated up to (a) 0, (b) 20, (c) 44, (d) 96, (e) 136, and (f) 180 kGy……..……49

Figure 3.13 Absorbance in characteristic bands and oxidation index values versus irradiation dose…….52
Figure 3.14 ^{1}H NMR spectra of the specimens irradiated up to (a) 0, (b) 96, and (c) 180 kGy.....53
Figure 3.15 ^{13}C NMR spectra of the specimens irradiated up to (a) 0, (b) 96, and (c) 180 kGy……54
Figure 3.16 DSC curves of the specimens irradiated up to (a) 0, (b) 20, (c) 44, (d) 96, (e) 136, and (f) 180 kGy……..……56
Figure 3.17 Effect of irradiation dose on the T_g values of the specimens……..58
Figure 3.18 DMA curves of the specimens irradiated up to (a) 0, (b) 20, (c) 44, (d) 96, (e) 136, and (f) 180 kGy.....60
Figure 3.19 Effect of irradiation dose on the T_g (tanδ peaks) of the specimens...62
Figure 3.20 TGA curves of the specimens irradiated up to (a) 0, (b) 96, and (c) 180 kGy…….64
Figure 3.21 TGA curves of the non-irradiated specimen (black line, denoted as NR), 96 kGy irradiated specimen (blue line) and 180 kGy irradiated specimen (red line)…….65

CHAPTER 1

INTRODUCTION

Ionizing radiation has been discovered to have remarkable effects on the structure and properties of polymeric materials. The molecular structure of polymers subjected to irradiation has been of interest since the early development of radiation chemistry in the 1950's, eventually resulting in the foundation of approximate guides to predict the alteration of properties. Some polymers particularly exhibit chain scissions while some of them become crosslinked under ionizing radiation. There can be circumstances where these effects are useful and ionizing radiation is used deliberately – this fact has led to the evolution and the increased use of various radiation processing techniques. Crosslinking of wire and cable insulation, curing of coatings and inks, vulcanization of natural and synthetic rubbers or other elastomers, sterilization of medical devices (vials, gauze, etc), controlled degradation of polymers like polypropylene and cellulosics, grafting of polymers such as acrylates onto fibers and fabrics, and the production of hydrogels are examples to the radiation processing applications [1, 2]. There may be cases where the effect of ionizing radiation is undesirable as well. In applications like space vehicles and nuclear power plants, polymeric materials are needed in environments of ionizing radiation due to various properties such as elasticity, light weight, formability etc. Such cases require polymeric materials that are as radiation resistant as possible [3]. All in all, how ionizing radiation affects polymers has long been an important issue in polymer research.

1.1 Polycarbonate

Polycarbonate (PC) is an engineering thermoplastic with characteristic properties of high strength, high toughness, high heat-deflection temperature and

transparency. It was discovered in 1898, and by the year 1958 both Bayer (Germany) and General Electric (USA) had started large scale production. Two synthesis processes have been extensively practiced, one of them being the interface process, which involves the reaction of bisphenol A with carbonyl chloride (phosgene). In the other method, transesterification of bisphenol A with diphenyl carbonate at high temperatures takes place. Both reactions are shown in Figure 1.1 [4].

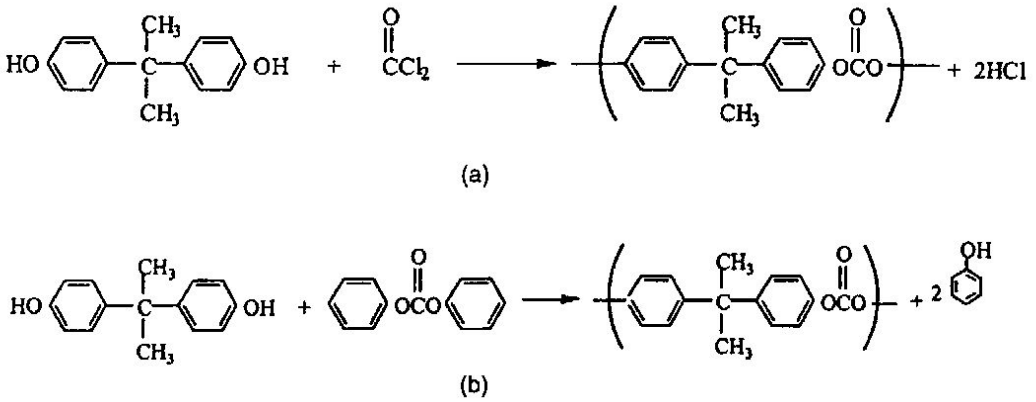

Figure 1.1 Synthesis reactions of polycarbonate: (a) interface process, and (b) transesterification reaction [4].

The carbonate segment in the molecular structure of polycarbonate is responsible for high toughness and ductility, and the bisphenol A segment provides high heat-deflection temperature. Additionally, polycarbonate is dimensionally stable and exhibits high creep resistance and good electrical properties [5].

Polycarbonate molding compounds have been produced for extrusion, injection molding, blow molding and rotational molding. Grades for film and sheet making with excellent optical and electrical properties are also available. Among the specialty grades, glass-reinforced polycarbonates have become attractive due to their improved tensile strength, tensile modulus, flexural modulus and chemical resistance [6].

Polycarbonate is utilized in a broad range of industries including electrical/electronics (small connectors, gears, etc), business machines, glazing, lighting applications, transportation applications (tail and sidemarker lights, traffic

light housings, etc), food contact applications (water bottles, baby formula bottles, tableware, food containers, etc), household appliances and so on [5].

Figure 1.2 Picture showing various items made from polycarbonate.

The use of polycarbonate in medical devices dates back approximately to its commercialization. Optical clarity is a critical property for clinical and diagnostic appliances in which visibility of tissues, blood and other fluids is necessary. In addition to these requirements, polycarbonate has proven successful in meeting the demands of biocompatibility standards as well [7]. Polycarbonate has turned out to be a suitable material in the production of certain medical devices like blood oxygenators, blood filters, anesthesia cannisters, inflators and centrifuge filter bowls [7,8].

In the medical market, sterilization is of extreme importance in the utilization of items that have direct contact with patients. Principal methods of sterilization are ethylene oxide (EtO) sterilization, irradiation, and steam autoclaving [7]. Irradiation, in which the material is exposed to ionizing radiation, is extensively employed among these methods.

Studies in which polycarbonate was evaluated as a candidate material to be utilized in the storage and disposal of radioactive waste also have been done [9].

These examples show that polycarbonate is a material that can encounter ionizing radiation in its areas of usage, thus an understanding of how the polymer behaves under irradiation is essential.

1.2 Ionizing Radiation and Its Interaction with Matter

Ionizing radiation, or high energy radiation, can be defined as all kinds of radiation with energies high enough to tear electrons apart from atoms or molecules. Ionizing radiation includes short wave electromagnetic radiations such as X-rays or gamma (γ)-rays, particulate radiations (α-particles, fast electrons, neutrons, protons, deuterons etc) and fission fragments. These radiations ionize the medium through which they pass, so they are commonly referred to as ionizing radiations. Although the energy range of these radiations is wide, the intensities are much higher than the bond dissociation energies [10]. Ionizing radiation is generated by radioactive materials, particle accelerators, X-ray tubes, and it also exists in the nature [11].

The different types of ionizing radiation may be classified according to the distance they penetrate through the material [12]. Neutrons and γ-rays are uncharged and can penetrate large distances through materials. β-particles and α-particles are charged particles and their penetration is much lower, β typically of the order millimeters whereas α only micrometers. In consequence, α-particles cause only surface effects; while neutrons, γ-rays and β-particles can irradiate the material more homogenously [13].

γ-rays are electromagnetic radiation of very short wavelength, about 0,01 Å for a 1 MeV photon [14]. γ-rays are emitted from many radioactive nuclei. Unstable atomic nuclei formed during nuclear transmutations often emit excess energy as γ-rays [12]. Sources from which γ-rays can be generated include ^{60}Co (1,17-1,33 MeV) or ^{137}Cs sources (0,66 MeV) [15].

Absorption of γ-rays by matter obeys the Lambert-Beer law:

$$I = I_0 e^{-\mu x} \qquad (1.1)$$

where I, I_0 are the intensities of the transmitted and incident radiations respectively, x is the thickness of the material absorbing the radiation and μ represents the linear absorption coefficient. The linear absorption coefficient is dependent on the density of the material and the mass absorption coefficient can be defined by:

$$\mu_{mass} = \mu_{linear}/\rho \quad (1.2)$$

where ρ denotes the density. The total absorption coefficient is the sum of three separate coefficients representing the three main processes by which γ-rays are absorbed in the material [14]:

i) Photoelectric effect: Photoelectric effect consists of the absorption of a photon by the electron cloud of an atom, resulting in the ejection of an electron, usually from an inner orbital of the atom. All the energy of the photon is used up in this process, and the energy of the emitted photoelectron is equal to the energy of the incident photon minus the binding energy of the electron. Photoelectric effect is the most important absorption process for photon energies below about 50 keV.

ii) Compton scattering: In Compton scattering, only a part of the photon energy is used to eject an orbital electron, and the remainder of the energy continues in the scattered photon. Compton scattering becomes less probable as the photon energy increases. It is thought that Compton scattering is the main absorption mechanism for photons having energies in the range of 100 keV-10 MeV.

iii) Pair production: In this process, an electron-positron pair is produced and subsequent annihilation of the positron generates γ-rays that may further interact by the first two processes. Pair production is can happen only if the photon energy is greater than 1,02 MeV [3, 16].

The amount of energy deposited in a medium by γ and other ionizing radiation is called the absorbed dose. The SI unit of absorbed dose is the gray, abbreviated

as Gy, which has units of (J/kg) and denotes the amount of radiation required to deposit 1 joule of energy in 1 kilogram of matter. The rad is the traditional unit of absorbed dose, equal to 0,01 joule deposited per kilogram, such that 100 rad = 1 Gy. Molecular changes created by the ionizing radiation are commonly characterized with a G value that quantifies the yield of an event. These events may be changes in molecular weight, gel content or other molecular alterations. The G value is defined as the event yield per 100 eV of absorbed energy. Most commonly, the G values are described for scission G(s), crosslinking G(x), and gas evolution G(g) [15].

1.3 Interaction of Ionizing Radiation with Polymers

Generally, the exposure of polymers to ionizing radiation brings change in their molecular structure and associated material properties. When ionizing radiation impinges on a polymeric material, the primary event is the ejection of a high energy electron:

$$R \rightarrow R^{+} + e^{-} \tag{1.3}$$

This primary electron can then cause ionization of other molecules, producing even more electrons. Consequently, a localized chain reaction of ionizations takes place:

$$e^{-} + R \rightarrow R^{+} + 2e^{-} \tag{1.4}$$

Because of Coulombic attraction, the positively charged ions produced disappear quickly as electrons recombine with them. The result of this process is the formation of highly excited electronic states:

$$R^{+} + e^{-} \rightarrow R^{*} \tag{1.5}$$

Additionally, a portion of the interactions of the radiation with the material can lead to energy transfer that is insufficient to cause ionization, but results directly in an electronically excited state of the molecule:

$$R \rightarrow R^* \quad (1.6)$$

The excited-state molecules may undergo radiationless decay to the ground state. In the mean time heat is produced, which can significantly raise the temperature of the sample. Depending on the particular molecular structures involved, the excited-states may decay by fluorescence or phosphorescence, thereby emitting light. Excited states can also decay by chemical reaction via bond cleavage leading to the formation of ions, or free radicals:

$$RX^* \rightarrow R\bullet + X\bullet \quad (1.7)$$

In spite of the fact that ions and excited-state molecules can directly yield chemical reactions, free radicals are the most effective agents in the radiation induced chemical processes in organic materials [3]. Following the creation of radicals a variety of processes can occur, these include:

i) Chain scission and crosslinking: The most important processes affecting the mechanical properties of irradiated polymers are those involving chain scission and crosslinking. Chain scission means the breakage of bonds causing the reduction of the molecular weight of the polymer, whereas crosslinking of molecules results in the formation of large three-dimensional molecular networks.

   Many polymers undergo both scission and crosslinking, but often one of these mechanisms predominates. Polymers subjected to irradiation in the absence of oxygen can be grouped into two categories, with reference to whether scission or crosslinking predominates. In general, polymers with a high concentration of tetra-substituted carbon atoms along the chain like polyisobutylene, poly(α-methylstyrene) and poly(methylmethacrylate) undergo primarily scission; polymers lacking this structural feature like polyethylene, polystyrene and poly(vinylchloride) undergo primarily crosslinking.

   Polymers which possess aromatic groups in their molecular structure are generally much more resistant to radiation induced crosslinking or

scission than aliphatic polymers regardless of the placement of the aromatic group on the chain. So, polystyrenes with a pendant aromatic group as well as polyimides with an aromatic group on the polymer backbone are relatively resistant to high doses of irradiation.

ii) Unsaturation and color changes: The formation of unsaturated sites is another important structural change that takes place upon irradiation. Double bonds are formed primarily due to loss of adjacent substituents on the chain or side group (e.g. adjacent H atoms in polyethylene) or to radical-radical termination reactions that occur by disproportionation.

Polymeric materials usually undergo color changes upon irradiation, because of the formation of conjugated, unsaturated chromophores or trapped radicals. Poly(vinylchloride) darkens (brown, red or black) at doses of 50-150 kGy and many polyolefins tend to yellow at doses around 100 kGy. Polystyrene and particularly polysiloxanes are resistant to color formation [3].

iii) Gas evolution: Gaseous species can be formed in the radiation degradation of polymers. Gas formation is a result of atom or side-chain abstraction and the nature of the gas closely reflects the composition of the macromolecule. The chemical nature of the gases is determined by that of the side groups in the repeating unit. In polyethylene the side groups are hydrogen, in poly(vinylchloride) they include chlorine, and in fluoropolymers they include fluorine. Thus, irradiation of these polymers will lead respectively to H_2, HCl and HF formation [3, 13, 17].

The Effects of Temperature, Mechanical Stress and Dose Rate

Different specimen temperatures can lead to differences in the chemistry of radiation induced degradation of polymers, mainly because of differences in radical mobility, with sharp changes often occurring near physical transition temperatures. Reduction in physical properties can proceed at an accelerated rate under the combined influence of applied stress and radiation. Possible

factors that are effective in radiation-stress interactions include weakening of certain bonds in macromolecules subjected to stress, and plasticization of the polymer by gaseous irradiation products.

It has been reported that under an inert atmosphere, the effect of radiation on polymers depend on the total absorbed dose and not on the dose rate [3].

The Effect of Oxygen

The presence of free radicals in the mechanism, which are highly reactive with oxygen, makes radiation-induced degradation highly sensitive to oxygen. The presence of oxygen strongly enhances the extent of degradation of many polymers, and the presence of oxygen after the irradiation may cause the same effect. Oxygen can react with the irradiated polymer to form initially peroxide and then hydroperoxide groups. Being thermally unstable, these hydroperoxide groups can spontaneously break down and produce further free radicals. In other words, the formation of hydroperoxide groups multiplies the number of radicals which would occur in the absence of oxygen. By this way the degradation is enhanced and, in many cases, extensive damage may occur at much lower absorbed doses than those required to cause pronounced changes under inert conditions [3, 10, 13].

If oxygen is present in the environment, the rate and the nature of degradation can be significantly dependent on the dose rate. The reasons for this are: (i) Oxygen diffusion may affect the mechanism, and (ii) steps in the oxidation mechanism may become rate-limiting on a time scale comparable to oxygen diffusion, peroxide breakdown, and free radical migration. Chemical reaction products include oxidized structures within the polymer, such as alcohol, ketone and carboxylic acid groups, as well as peroxidic species. Gaseous products include those are formed upon irradiation under inert conditions, together with significant amounts of CO, CO_2, and H_2O [3].

1.4 Effects of Ionizing Radiation on Polycarbonate

Studies on the effects of ionizing radiation on polycarbonate dating back to almost 1950's can be found in the literature. Some of these studies are summarized below.

• Golden and Hazell irradiated Lexan® polycarbonate by using electron beams both in oxygen and vacuum up to a dose of 1000 Mrad [18]. Irradiated specimens were found to be soluble in methylene chloride and chloroform at all doses used, the ease of dissolution increasing with the dose. Since no gel formation was observed, it was suggested that crosslinking did not take place and main chain scission was the major effect of irradiation. Molecular weight values measured on the irradiated specimens supported this conclusion. A progressive decrease in the viscosity average molecular weight (M_v) with increasing dose both in vacuum and oxygen was observed. The presence of oxygen had a slight accelerating effect on the degradation. The maximum yield strength and elongation decreased slowly until a dose of approximately 100 Mrad, and once this dose was exceeded the maximum yield strength fell rapidly and the elongation became extremely low. The authors also reported that the change in modulus with dose within the studied range was negligible.

The colors of the irradiated specimens were observed to change from transparent to brownish-black as the dose increased. This darkening in color was accompanied with an increased UV light absorption of the irradiated material, which was ascribed to the formation of conjugated unsaturation in the carbonyl groups.

Mass spectroscopic analyses of the specimens irradiated either in vacuum or in oxygen after a dose of 1000 Mrad revealed the existence of CO, CO_2, H_2 and O_2 in the order of decreasing amount. Both CO and CO_2 were said to have arisen from the destruction of the carbonate linkage.

• Golden et al. examined the effect of radiation dose and molecular weight on the tensile and flexural properties of polycarbonate [19]. Bars machined from Makrolon® Grade S polycarbonate sheet were irradiated with several doses up to

240 Mrad. The tensile and flexural strength decreased, while the flexural modulus increased linearly with increasing dose up to 80 Mrad. The reciprocal viscosity average molecular weight increased clearly with increasing dose up to 240 Mrad. The forms of the tensile and flexural yield strength curves were remarked to be representing the dependence of these parameters on the molecular weight.

• Torikai et al. investigated the γ-degradation behavior of polycarbonate by electron spin resonance (ESR) and molecular weight determinations [20]. They subjected films of Panlite® polycarbonate to γ-irradiation in vacuum or in air at -196 °C or 25 °C. Films irradiated at -196 °C gave an ESR spectrum which could be assigned to trapped electrons, phenyl and phenoxy type radicals. The molecular weight decreased with increasing irradiation dose both in vacuum and in air. Also examining the infrared (IR) spectra of γ-irradiated specimens, the authors suggested a mechanism for the degradation of polycarbonate. In the presence of air, the radicals formed upon irradiation might react with oxygen to form peroxy radicals, which are then converted into oxygenated products, paving the way to the degradation of the polymer. The authors concluded that irradiation of polycarbonate films results mainly in chain scissions.

• Babanalbandi et al. carried out a study on the γ-irradiation behavior of a polyarylate (product of Unitake) and polycarbonate (product of Aldrich) using spectroscopic techniques [21]. In the nuclear magnetic resonance (NMR) study, the samples irradiated at ambient temperature were subjected to doses of 4 and 10 MGy and those irradiated at 423 K were subjected to a dose of 1 MGy. No detectable changes appeared in the ^{13}C NMR spectrum of polycarbonate irradiated at ambient temperature. Comparing the spectra of the non-irradiated and irradiated samples of polycarbonate, the authors noticed that some new peaks were formed on irradiation at 423 K. The observed changes were also consistent with the fact that the destruction of carbonate or ester linkages is the main effect, CO and CO_2 being the principal gaseous products formed by the degradation of carbonate groups on the chain.

• In their study on the radiolytic degradation and stability of polycarbonate, Arajuo and Guedes did not observe any change between the ^{1}H NMR spectra of Durolon® polycarbonate samples that were non-irradiated and irradiated to 250

kGy [22]. The ESR study revealed that phenoxy and phenyl radicals were formed upon irradiation. The authors explained the yellowish appearance of the irradiated samples by the presence of long-lived phenoxy radicals.

• Acierno et al. observed the γ-irradiation effects on a Lexan® polycarbonate by making rheological and dynamic mechanical analyses [23]. Samples cut from sheet were irradiated at room temperature and in air within the range 0-20 Mrad. An initial decrease and a following increase in the melt flow index (accompanying an initial increase and a following decrease in the intrinsic viscosity) with increasing dose was observed. This behavior was attributed to a molecular weight increase of approximately 15% at the dose level corresponding to the minimum of the melt flow index (4 Mrad). The authors considered such an amount of increase in molecular weight at low doses as a simple branching and not a real crosslinking.

In the dynamic mechanical analyses of this study, the strong peak on the loss modulus (*E"*) versus temperature curve was obtained at about 145 °C and this peak moved slightly to lower temperatures with the increasing dose. Both on the loss modulus (*E"*) versus temperature and the dissipation factor (tanδ) versus temperature curves a weak new peak at around 100 °C appeared as the dose increased. The authors reminded that at these dose levels scissions on a branched structure decrease the size of the pendant groups and increase the number of small molecules, and suggested that the presence of the new peak might be explained by relaxation behavior of these units.

• Kalkar et al. subjected bisphenol A polycarbonate films to various irradiation doses at room temperature in air [24]. The glass transition temperature (T_g), as determined by differential thermal analysis (DTA), decreased very rapidly up to a dose of 0,15 MGy and then there appeared a somewhat more gradual decrease. The T_g of polycarbonate was observed to decrease from 422 K for non-irradiated samples to 407 K for the sample irradiated up to the maximum dose (0,68 MGy). This wide variation in T_g were attributed to the increase in excess free volume which was a result of random chain scission caused by the irradiation. The bands that were representative of the carbonate group (at 1790 cm^{-1}) and the methyl

group (at 2969 and 1230 cm^{-1}) vibrations on the Fourier-transform infrared (FTIR) spectra were the most affected bands in polycarbonate due to irradiation.

• In order to investigate the γ-irradiation effects on Durolon® polycarbonate, Arajuo et al. carried out a study that incorporated molecular weight measurements, tensile and impact tests, FTIR spectroscopy studies and yellowness index measurements on irradiated specimens [25]. Polycarbonate in the form of test specimens was irradiated at room temperature in air within the range 0-300 kGy. γ-irradiation was found to result in main chain scission, causing a decrease in molecular weight of the polymer. However, this degradation was not sufficient to significantly change the mechanical properties of Durolon®, up to 100 kGy. This observation was compared with those that had been previously reported for Lexan® and Merlon® polycarbonates. When irradiated under similar conditions as Durolon®, Lexan® had been reported to exhibit a crosslinking effect at low doses while at higher doses main chain scission was more predominant [RA50]. Merlon® polycarbonate, when irradiated, showed the same behavior as Durolon® [26]. A comparative analysis of these three polycarbonates regarding the effect of γ-irradiation on their intrinsic viscosity showed that the intrinsic viscosity of Lexan® first increased then decreased with increasing dose, displaying a peak value at around 40 kGy. The maximum intrinsic viscosity values of Merlon® and Durolon® belonged to their non-irradiated samples and these values clearly decreased with increasing dose. It was noted that polycarbonates might exhibit different behavior when they were subjected to γ-irradiation under different conditions.

The decrease in the absorption of carbonyl band with the increase of radiation dose in the FTIR spectra of Durolon® irradiated up to different doses confirmed the remarks by previous authors that carbonyl groups were the sites at which main chain scissions take place. The carbonyl index, which was determined by the ratio A_{1771}/A_{758} where A_{1771} was the intensity of the C=O stretch band and A_{758} was the intensity of out-of-plane bending absorption of the C–H bond of the rings (regarded to be proportional to the amount of sample that was not affected by irradiation), displayed a steady decrease as the irradiation dose increased.

• De Melo et al. investigated the behavior of polycarbonate specimens before and after γ-irradiation by carrying out molecular weight measurements, FTIR spectroscopy and mechanical tests [27]. Specimens of Lexan® Margard polycarbonate were subjected to doses varying between 25 and 125 kGy at room temperature in air. The viscosity average molecular weight of the specimens, as determined by dilute solution viscometry using chloroform as the solvent, were found to increase slightly for the lowest dose (25 kGy) and then decrease more severely as the absorbed dose increased. This behavior suggested a crosslinking effect for small doses, and chain scission at higher doses. Also taking into account the statements in the literature that radiation induced scission takes place at carbonate groups accompanied by the formation of gases like CO, CO_2 and H_2, the authors concluded that γ-irradiation causes a decrease in the molecular weight of polycarbonate.

FTIR study was also carried out. Similar to the carbonyl index definition used by Arajuo et al. [25], the authors calculated the oxidation index as the ratio of the peak height at 1775 cm^{-1} (A_{1775}), corresponding to C=O carbonyl stretching, to the peak height at 769 cm^{-1} (A_{769}), corresponding to C-H out-of-plane bending of the aromatic ring. The change of the absorbance intensity of the 1775 cm^{-1} band as the absorbed dose increased suggested that the carbonyl group is prone to the effect of γ-irradiation, and that chain scission starts with the breaking of C=O bonds. The FTIR results were accepted to be confirming that chain scission occurs mainly in the carbonyl group.

• Sinha et al. studied γ-induced modifications in polycarbonate (product of Bayer AG) in the dose range of 10^1-10^6 Gy [28]. The glass transition temperature (T_g) of the irradiated specimens, as determined by differential scanning calorimetry (DSC), decreased with increasing dose from 151,8 °C for the non-irradiated specimen to 140 °C for the dose of 10^6 Gy.

• Sinha and Dwivedi investigated the effect of γ-irradiation on the thermal properties of nuclear track detectors made from different type of polymers in the dose range of 10^1-10^6 Gy[29]. Thermogravimetric analysis (TGA) of irradiated polycarbonate detectors showed single-step decompositions up to the dose of 10^5 Gy and a a two-step decomposition at 10^6 Gy. In all detectors that were irradiated

up to 10^5 Gy, the decomposition started around 480 °C and ended around 570 °C with total weight losses of approximately 70%. But in the detector that was irradiated up to 10^6 Gy, weight loss started around 420 °C and continued up to 700 °C. At 700 °C, 7% of the total weight remained. This indicated that up to a dose of 10^5 Gy, the stability was retained after first decomposition (above 570 °C), but when the irradiation dose was increased to 10^6 Gy the stability was lost above 570 °C and the weight loss continued up to 700 °C.

1.5 The Aim of This Study

This study aims to determine how ionizing radiation affects polycarbonate. This is accomplished by applying different doses of gamma radiation to the injection molded samples of the polymer and employing various characterization techniques to reveal any changes brought by irradiation. This thesis is also a part of continuing research on the effect of gamma radiation on the properties of polymers in our laboratory. Previously, the effects of gamma radiation on various polymers have been studied and the results have been published [30-34].

CHAPTER 2

EXPERIMENTAL PROCEDURE

2.1 Material

The material used in this study was Lexan® LS2 resin, product of GE Plastics (now a branch of SABIC, a Saudi Arabian petrochemicals company). As described by the producer, this is a medium viscosity grade specifically suitable for applications requiring high clarity and light transmission. The resin granules can be seen in Figure 2.1.

Figure 2.1 Granules of polycarbonate used in this study.

2.2 Shaping of the Specimens

The granules were shaped into dog bone specimens (for the aim of tensile testing) and rectangular bar-shaped specimens (for the aim of flexural testing and dynamical mechanical analyses) by injection molding. A small scale industrial

type injection molding machine (Permak Baby Plast), as shown in Figure 2.2 was used. The injection pressure was 80 bars, the barrel temperature was around 280 °C and the mold temperature varied between 25-45 °C. The dimensions of the dog bone specimens confirmed the specifications of ISO 527-1 standard, and those of the bar-shaped specimens confirmed the specifications of ISO 178 standard. Figure 2.3 displays both type of specimens produced.

Figure 2.2 Injection molding machine used for shaping of the specimens.

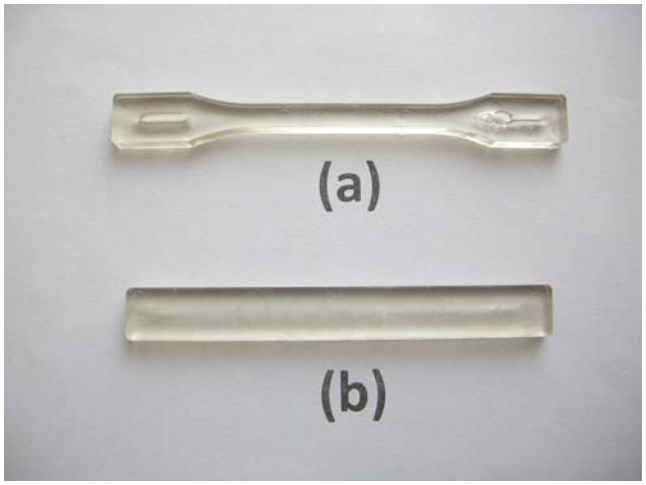

Figure 2.3 (a) Dog bone, and (b) bar-shaped specimen.

2.3 Irradiation of the Specimens

After the shaping of the specimens by injection molding, the next experimental step was the irradiation operation. Specimen groups each containing sufficient numbers of dog-bone and bar-shaped specimens as well as unshaped resin granules were irradiated by using a Tenex Issledovatel model ^{60}Co γ-source with a dose rate of 0,8 kGy/h in the presence of oxygen. Irradiations were carried out at the Sarayköy Nuclear Research and Training Center of the Turkish Atomic Energy Authority (TAEK). At the end of irradiations, specimen groups each had absorbed a different total dose (20, 44, 96, 136 and 180 kGy) were obtained.

In the next experimental step, various tests and analyses were conducted on both irradiated and non-irradiated specimens, in order to investigate the effects of irradiation.

2.4 Mechanical Tests

The effect of irradiation on the mechanical behavior of polycarbonate was examined by conducting (i) tensile tests (ISO 527-1), (ii) three-point bending tests (ISO 178), and (iii) hardness tests (Shore D).

2.4.1 Tensile Tests

In a tensile test, the specimen is extended along its major longtidunal axis until the specimen breaks or until the stress (load) or the strain (elongation) attains some predetermined value. During the test, the load sustained by the specimen and the elongation are measured [35].

The (engineering) tensile stress is defined as the tensile force per unit cross-sectional area within the gauge length, acting on the specimen at any given moment:

$$\sigma = \frac{F}{A_0} \tag{2.1}$$

The (engineering) tensile strain is defined as the increase in length per unit original length of the gauge:

$$\varepsilon = \frac{\Delta l}{l_0} \tag{2.2}$$

The ratio of stress to strain within the elastic region, where the change of stress with respect to strain is linear, gives the tensile modulus:

$$E = \frac{\sigma}{\varepsilon} \tag{2.3}$$

2.4.2 Bending Tests

The procedure of a (3-point) bending test consists of the deflection of the test specimen at a constant rate at the midspan until the specimen breaks or until the deformation reaches a certain value. During the experiment, the force applied to the specimen and the deflection experienced by the specimen are measured [36].

The flexural stress is defined as the nominal stress of the outer surface of the test specimen at the midspan, and it is calculated by the formula:

$$\sigma_f = \frac{3FL}{2wt^2} \tag{2.4}$$

where F denotes the load, L denotes the span length, w denotes the specimen width and t denotes the specimen thickness.

The flexural strain is defined as the nominal fractional change in length of an element of an outer surface of the test specimen at midspan, and it is calculated by the formula:

$$\varepsilon_f = \frac{6\Delta dt}{L^2} \tag{2.5}$$

where Δd denotes the deflection of the specimen, which is the distance over which the top or bottom surface of the specimen at midspan has displaced from its original position.

The flexural modulus, E_f, is calculated in a similar manner to the calculation of the tensile modulus.

The tensile and bending tests in this study were done by using a computer controlled Lloyd Instruments LR 5K model testing machine with a load cell of 5 kN. A constant crosshead speed of 1 mm/min in tensile tests and 2 mm/min in bending tests were used. Figure 2.4 shows specimen gripping and supporting during tensile and bending tests.

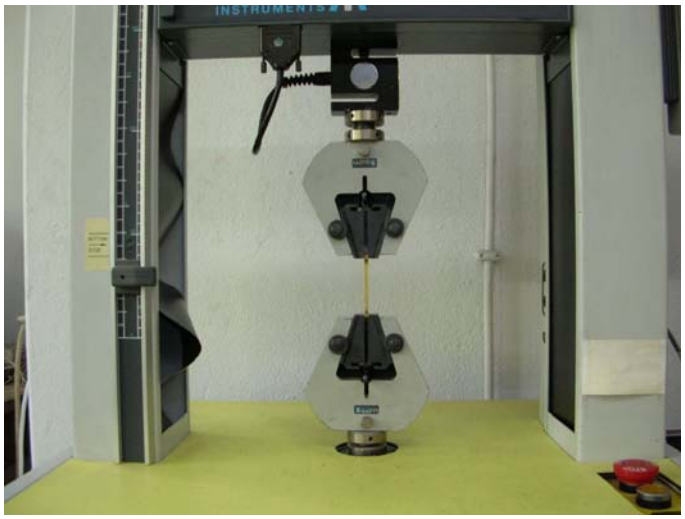

(a)

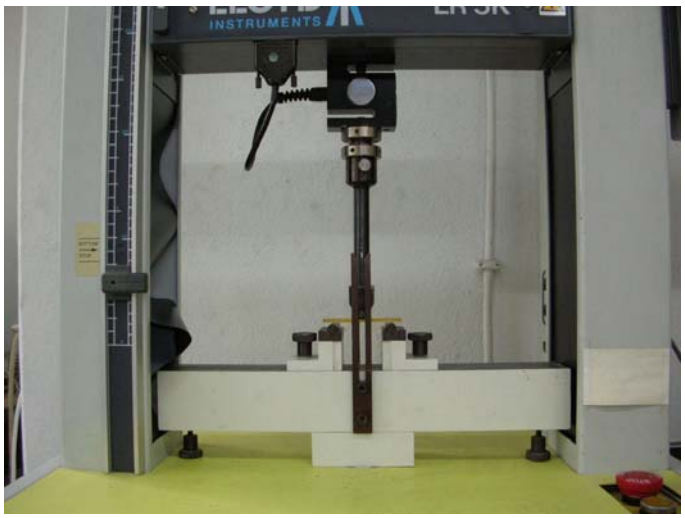

(b)

Figure 2.4 Specimen gripping and supporting during (a) tensile, and (b) bending tests.

Tensile tests were performed on 7 specimens from each group having the same absorbed dose. Regarding the behavior of the specimens during the test and the results obtained, 5 tests were selected in each group and 2 were discarded. Bending tests were performed on 5 specimens from each group having the same level of absorbed dose. The specimens did not break under bending, therefore the tests were terminated manually just after reaching the maximum value of the load.

2.4.3 Hardness Tests

Hardness can be roughly described as the resistance of a material to indentation. Almost all hardness test methods regard the size of an indent formed by an indentor in the material as an indication of its hardness: the smaller the indent produced, the harder the material, and so the greater the hardness number [37].

One of the most common techniques for measuring the hardness of polymeric materials is the Shore hardness, sometimes referred to as Shore durometer hardness. The technique has two main variants, Shore A and Shore D. Shore A scale is suitable for soft plastics while Shore D is suitable for harder plastics. Shore durometers are small, hand-held instruments with indentors of definite geometry that are pressed into the surface of the test piece to be measured under a spring of a given stiffness. The amount of penetration of the indentor is measured by a suitable scale marked directly in hardness degrees [38].

A Shore D durometer, as illustrated in Figure 2.5, was used to measure the hardness of both non-irradiated and the irradiated specimens. The rectangular bar-shaped specimens were used, and the hardness values were read directly on the dial gauge of the instrument. Seven measurements were taken from each specimen and the averages of these measurements were calculated.

Figure 2.5 Shore D durometer used in hardness measurements.

2.5 Molecular Weight Determinations

The effect of radiation dose on the molecular weight was studied by both dilute solution viscometry and gel permeation chromatography.

2.5.1 Dilute Solution Viscometry

Dilute solution viscometry is a technique based on the fact that polymer molecules are able to increase the viscosity of the liquid in which they are dissolved, even when present at quite low concentrations. As the molecular weight of a linear polymer gets higher, the increase in viscosity produced by a given concentration of that polymer becomes greater. Although an absolute value for the molecular weight of a polymer cannot be derived from solution viscosity measurements, the simplicity of the measurement and the usefulness of the viscosity-molecular weight correlation are so great that the technique is one of the most commonly employed ones in the molecular characterization of polymers [39-40].

Solution viscosity measurements generally involve the comparison of the efflux time t during which a certain volume of polymer solution flows through a capillary tube to the corresponding efflux time t_0 of the solvent. From t, t_0 and the solute concentration, several parameters are derived to be used in viscosity studies. The relative viscosity, $\eta_r = \eta / \eta_0$, is the viscosity of the solution η relative to that of the pure solvent η_0. Viscosity of a solution depends on density and flow time. But if i)

the density of solution is equal to the density of solvent, ii) flow time is more than 90 seconds, and, iii) solution is dilute; the viscosity depends only on flow time. So, the relative viscosity can be written as $\eta_r = \eta / \eta_0 = t / t_0$. The specific viscosity, $\eta_{sp} = (\eta - \eta_0) / \eta_0 = \eta_r - 1$, represents the fractional increase in the viscosity resulting from the dissolved polymer in the solvent. The reduced viscosity, $\eta_{red} = \eta_{sp} / c$, is the increase in solution viscosity per unit of polymer solute concentration, c. It is a measure of the capacity of a given polymer to enhance the specific viscosity. The intrinsic viscosity, [η] represents the intrinsic ability of a polymer solute to increase the viscosity of a particular solvent at a given temperature. The intrinsic viscosity is the limit of the reduced viscosity, and also the limit of the inherent viscosity $\eta_{inh} = (\ln \eta_r) / c$ as the solution polymer concentration approaches zero.

$$[\eta] = [(\ln \eta_r) / c]_{c=0} \tag{2.6}$$

Extrapolation to infinite dilution of the viscosity data as a function of concentration is accomplished by means of the Huggins equation

$$\eta_{red} = \eta_{sp} / c = [\eta] + k' [\eta]^2 c \tag{2.7}$$

or the Kreamer equation

$$\eta_{inh} = (\ln \eta_r) / c = [\eta] + k'' [\eta]^2 c \tag{2.8}$$

where k' and k'' are constants. By taking measurements at a number of concentrations, either the reduced viscosity or the inherent viscosity can be graphically extrapolated to zero concentration to obtain the intrinsic viscosity.

The intrinsic viscosity measured in a specific solvent is related to the viscosity average molecular weight, M_v, in terms of the Mark-Houwink equation

$$[\eta] = K (M_v)^a \tag{2.9}$$

where K and a are Mark-Houwink constants that depend upon the type of polymer, solvent, and the temperature. One can determine these constants

experimentally, or refer to the literature to see whether they have been determined for the specific experimental conditions and published before. Detailed tables of Mark-Houwink constants for most commercially important polymers are accessible. Thus, once the intrinsic viscosity of a polymer is known, the viscosity average molecular weight can be calculated by the use of Mark-Houwink equation.

In this study, the intrinsic viscosities of both non-irradiated and irradiated specimens dissolved in tetrahydrofuran (THF) were measured using an Ubbelohde type viscometer in a circulated water bath at 25 °C, and the viscosity average molecular weights were calculated thereafter.

2.5.2 Gel Permeation Chromatography

Gel permeation chromatography (GPC) is an analytical method which enables the determination of the average molecular weight and the molecular weight distribution of polymers. A GPC device consists of columns packed with porous beads, the size of the pores being comparable to the dimensions of polymeric sample to be analyzed. During operation, pure solvent is pumped through the GPC columns, and then a small amount (1-5 mL) of polymer solution is injected into the stream passing through the beads. Smaller molecules of the polymeric sample can penetrate into the pores more easily and are therefore retained inside the column to a greater extent than the larger molecules. Larger molecules continue their way in the stream and elute out of the column faster. So, the molecules exit the column in order of their size, the largest emerging first. Separation according to the molecular size is accomplished by this way, and through the use of proper monitoring tools and calibration curves the average molecular weights and the molecular weight distribution can be figured out [40-43].

Gel permeation chromatography analyses of this study were done on a Polymer Laboratories PL-GPC 220 device at room temperature. The solvent was again THF, and the results were interpreted using polystyrene universal calibration method.

2.6 Spectroscopic Analyses

Infrared spectroscopy and nuclear magnetic resonance spectroscopy were the techniques used to examine whether any change in the molecular structure of the polymer had taken place or not.

2.6.1 Infrared Spectroscopy

Infrared (IR) spectroscopy is a technique of characterization of the molecular structure based on the vibrational behavior of specific bonds under the effect of electromagnetic radiation in the infrared range. Different vibrational modes exhibit different absorbance characteristics. So, by passing infrared radiation through a sample and measuring the fractions of the energy that is absorbed at different wavelengths, a spectrum showing the absorbances of characteristic vibrational modes can be obtained, which informs about the existence of the corresponding bonds in the sample [44].

The specimens analyzed in infrared spectroscopy are usually in the form of pressed or cast films. Reflectance methods, such as ATR (attenuated total reflectance) enable bulk specimens or surfaces to be examined.

The IR spectra of the specimens in this study were recorded on a Thermo Scientific Nicolet iS10 model ATR-FTIR spectrometer. The measurements were done in the wavenumber range 400-4000 cm^{-1}, and the resolution was 4 cm^{-1}.

2.6.2 Nuclear Magnetic Resonance Spectroscopy

Nuclear magnetic resonance (NMR) spectroscopy is the study of the molecular structure by measuring the interaction of an radiofrequency radiation with certain nuclei of the atoms in the sample placed in a strong magnetic field. An atomic nucleus, when placed in a magnetic field, tends to align with the applied field. The energy required to reverse this alignment is quantized and it depends both on the magnitude of the magnetic field and the environment of the nucleus, that is, the nature of the chemical bonds between the atom of interest and its neighboring atoms. By observing the energy levels of transition for the atoms that exhibit such

a reversal, it is possible to determine the presence and bonding characteristics of these atoms. The energy levels can be expressed in terms of frequency of the radiation. The minor spectral shifts created by the chemical environment are the essential features for interpreting the structure. These are generally expressed in terms of ppm shifts (denoted as δ) from the frequency of a reference compound such as tetramethylsilane (TMS).

NMR spectroscopy utilizes nuclei with a spin number equal to ½, such as ^{1}H, ^{13}C, ^{19}F and ^{31}P. ^{1}H and ^{13}C are the most commonly examined nuclei by NMR, since they are the NMR sensitive nuclei of the most abundant elements in organic materials [44, 45].

In this study, ^{1}H and ^{13}C nuclear magnetic resonance (NMR) spectra of the specimens of selected doses were taken on a Bruker Ultrashield 400 model device using deuterated chloroform ($CDCl_3$) as the solvent and tetramethylsilane (TMS) as the reference compound.

2.7 Thermal Analyses

The effect of irradiation on the thermal properties of the polymer was investigated by differential scanning calorimetry, dynamic mechanical analysis and thermogravimetric analysis.

2.7.1 Differential Scanning Calorimetry

Differential scanning calorimetry (DSC) is a method in which the energy required to keep the temperature of the sample and a reference material the same with changing temperature or time is measured. The basic principle underlying DSC is that in case a physical transformation takes place in the sample, more or less heat will be required to flow to it than the reference material to maintain both at the same temperature, depending on whether the transformation is endothermic or exothermic. For example, melting of a solid sample requires more heat flowing to the sample as to increase its temperature at the same rate as the reference, and the transition appears as an endothermic peak on the DSC curve. DSC enables also the observation of phase changes like glass transitions. The glass

transition temperature (T_g) of a polymer, which is accompanied by a change in the heat capacity of the material, creates an endothermic shift in the baseline of the DSC curve. Consequently, by examining DSC curves the temperature at which a particular transition takes place as well as the associated enthalpy change can be determined [44, 46].

In the DSC study of this thesis, small aluminum pans containing the specimens were prepared and the thermograms were taken on a Scinco DSC N-650 model differential scanning calorimeter between 25-325 °C with a heating rate of 10 °C/min, using empty aluminum pans as the reference and N_2 as the protective atmosphere.

2.7.2 Dynamic Mechanical Analysis

Dynamic mechanical analysis (DMA) is a technique used to determine the elastic modulus of a material and its mechanical damping or energy dissipation characteristics as a function of frequency and temperature. In DMA, a sinusoidal stress is applied to the material and the resulting strain is measured. As a result of time-dependent relaxation processes, a consequence of the viscoelastic behavior of the material, the strain lags behind the stress. For a frequency of oscillation ω, the stress σ, at any given time t, can be represented as:

$$\sigma = \sigma_0 \sin(\omega t + \delta) \tag{2.10}$$

where σ_0 is the maximum stress and δ is the phase angle which is equal to the amount of lag between the stress and strain. The strain, ε, is given by:

$$\varepsilon = \varepsilon_0 \sin\omega t \tag{2.11}$$

The stress can be resolved into two parts, one being in-phase and the other being 90° out-of-phase with the strain. Two tensile moduli can also be defined, denoted as *E'* and *E"* and named the storage modulus and the loss modulus, respectively. The storage modulus is proportional to the recoverable energy, whereas the loss modulus is proportional to the energy dissipated as heat. The tensile storage and loss moduli can be represented as:

$$E' = (\sigma_0 / \varepsilon_0) \cos\delta \quad (2.12)$$

$$E'' = (\sigma_0 / \varepsilon_0) \sin\delta \quad (2.13)$$

The dissipation factor, or tanδ can be obtained from the division of the loss modulus into the storage modulus:

$$\tan\delta = E'' / E' \quad (2.14)$$

DMA is a technique which enables the determination of the glass transition temperature (T_g) of polymers. When the analysis is carried out at fixed frequency and variable temperature (sometimes referred to as temperature sweep mode), the storage modulus decreases significantly and the loss modulus reaches a maximum at the glass transition, creating a peak value in tanδ [44, 47].

Dynamical mechanical analyses in this study were carried out on a TA Instruments DMA 983 model dynamical mechanical analyzer in bending mode. Bar-shaped specimens of dimensions 80x10x4 mm^3 were used. Under N_2 atmosphere, the temperature range between 20 °C and 200 °C was scanned with a heating rate of 2 °C/min while the oscillation frequency was kept constant at 1 Hz.

2.7.3 Thermogravimetric Analysis

Thermogravimetric Analysis (TGA) is a thermal analysis method which incorporates the measurement of weight loss of a sample as a function of temperature or time. By this method, the change in mass of a polymer caused by transitions or degradation processes can be determined quantitatively. The analysis is performed by increasing the temperature of the sample gradually and detecting the change in weight. The TGA curve can be drawn as the weight loss as a function of temperature, or alternatively, in a differential form where the change in sample weight with time (derivative weight) is plotted as a function of temperature [44].

Thermogravimetric analyses of the specimens of selected doses in this study were done by a Perkin Elmer Pyris 1 model thermogravimetric analyzer in the temperature range 25-900 °C with a heating rate of 10 °C/min under N_2 atmosphere.

CHAPTER 3

RESULTS AND DISCUSSION

3.1 Discoloration

After the irradiations were complete, specimens that had absorbed different doses were visually inspected and compared with each other. As can be noticed in Figure 3.1, the irradiated specimens turned into yellow and the color darkened as the absorbed dose increased. Although no experimental evidence is presented in this study, the reason for this color change has been explained by various authors in the literature by the formation of phenoxy and phenyl radicals [22], or unsaturation [18] in polycarbonate upon irradiation.

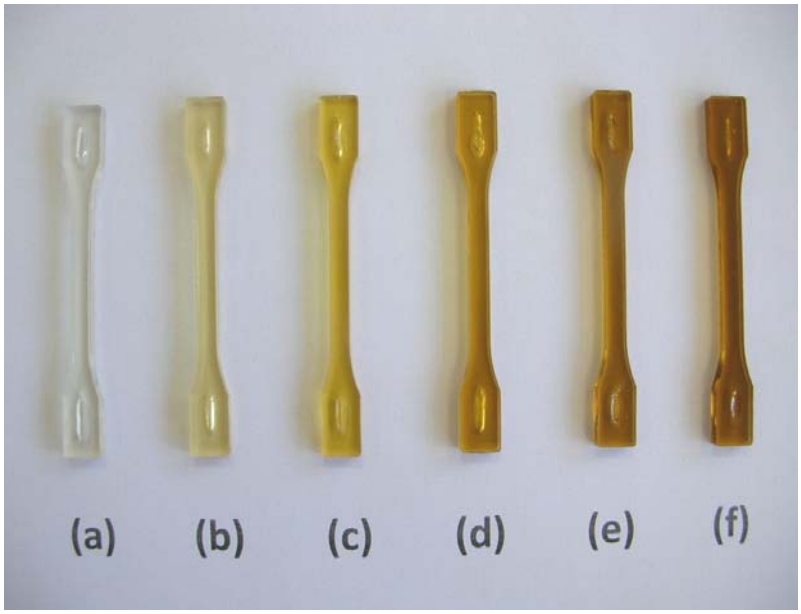

Figure 3.1 Color change observed after irradiation doses of (a) 0, (b) 20, (c) 44, (d) 96, (e) 136, and (f) 180 kGy.

3.2 Effects on the Mechanical Properties

3.2.1 Tensile Tests

Representative tensile stress-strain curves from each specimen group are given in Figure 3.2.

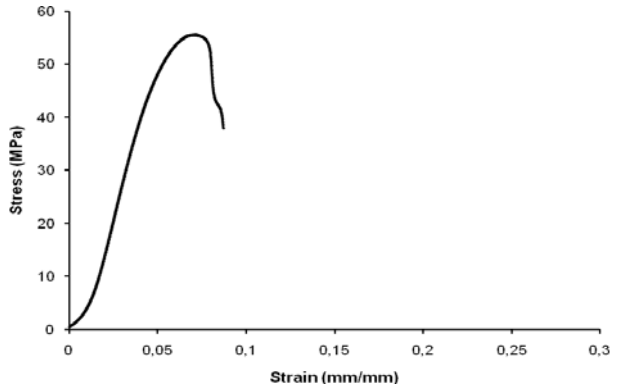

(a)

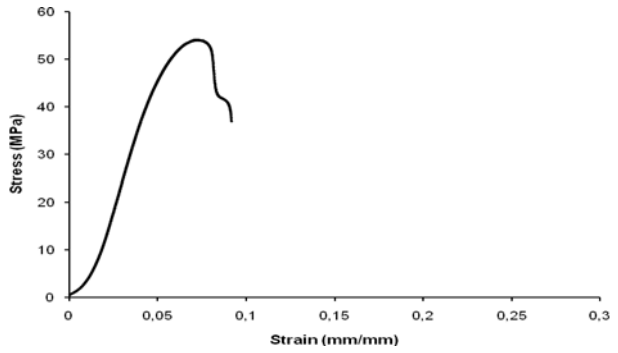

(b)

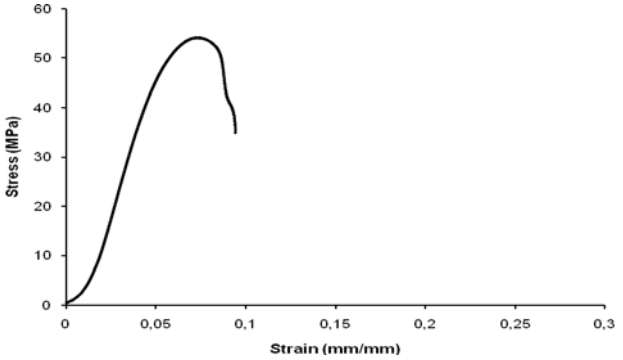

(c)

Figure 3.2 Representative tensile stress-strain curves of the specimens irradiated up to (a) 0, (b) 20, (c) 44, (d) 96, (e) 136, and (f) 180 kGy.

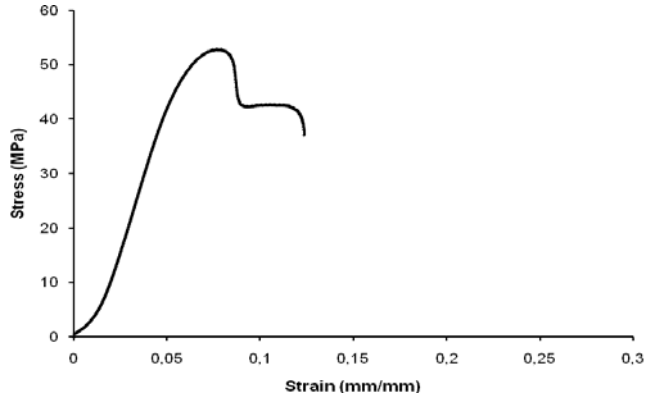

(d)

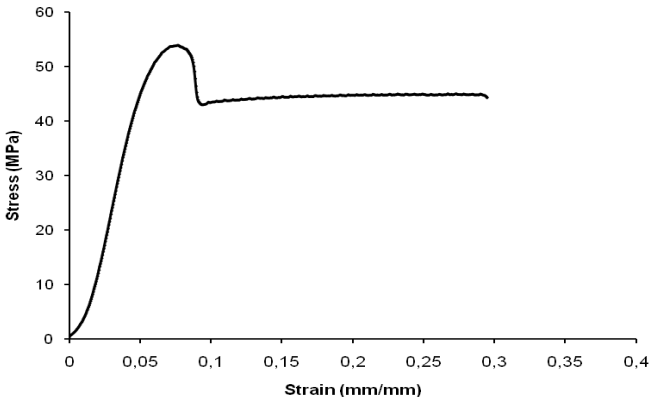

(e)

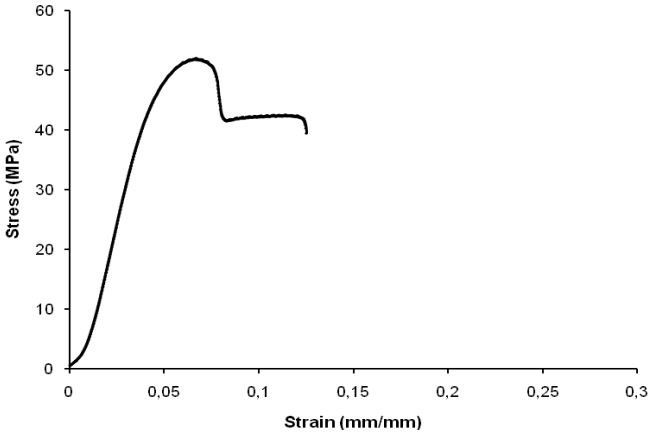

(f)

Figure 3.2 Representative tensile stress-strain curves of the specimens irradiated up to (a) 0, (b) 20, (c) 44, (d) 96, (e) 136, and (f) 180 kGy (cont'd).

The slope of the linear (elastic) portion on each stress-strain curve was calculated and recorded as the tensile modulus value. The maximum stress attained on each

curve was recorded as the tensile strength value. The values obtained from all specimens are given in Tables 3.1 and 3.2.

Table 3.1 Tensile modulus values of the test specimens

	Tensile Modulus (MPa)					
Absorbed Dose (kGy)	Specimen 1	Specimen 2	Specimen 3	Specimen 4	Specimen 5	Average
0	1355	1313	1276	1338	1324	1321 ± 30
20	1316	1277	1322	1272	1321	1302 ± 25
44	1283	1200	1390	1368	1283	1305 ± 76
96	1122	1293	1141	1429	1401	1277 ± 142
136	1424	1245	1204	1383	1431	1337 ± 106
180	1449	1454	1322	1324	1399	1390 ± 64

Table 3.2 Tensile strength values of the test specimens

	Tensile Strength (MPa)					
Absorbed Dose (kGy)	Specimen 1	Specimen 2	Specimen 3	Specimen 4	Specimen 5	Average
0	55,6	55,5	54,9	54,8	55,6	55,3 ± 0,4
20	55,5	54,1	54,6	54,9	55,4	54,9 ± 0,6
44	54,2	53,6	54,8	54,8	54,2	54,3 ± 0,5
96	52,9	54,3	53,6	54,2	53,3	53,6 ± 0,6
136	54,2	53,9	53,2	53,1	53,2	53,5 ± 0,5
180	52,9	53,0	52,6	51,8	52,0	52,5 ± 0,5

The effect of irradiation dose on the tensile modulus and the tensile strength are evaluated in Figures 3.3 and 3.4.

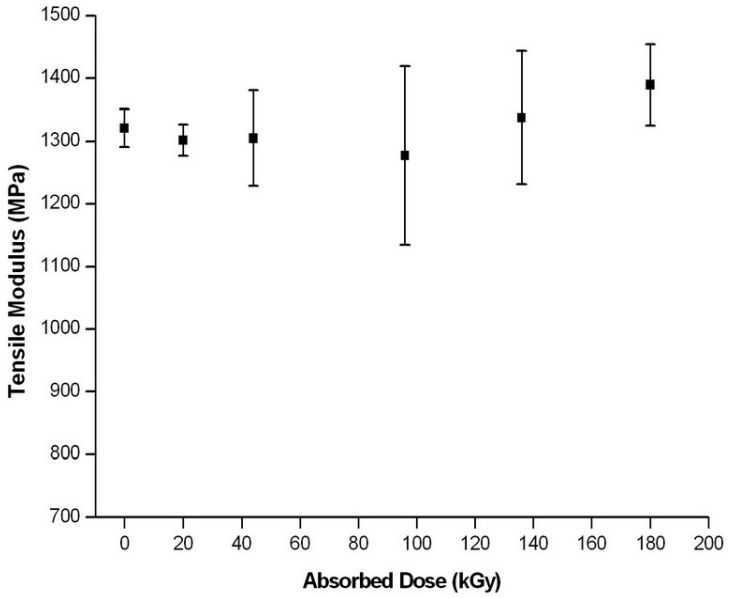

Figure 3.3 Effect of irradiation dose on tensile modulus.

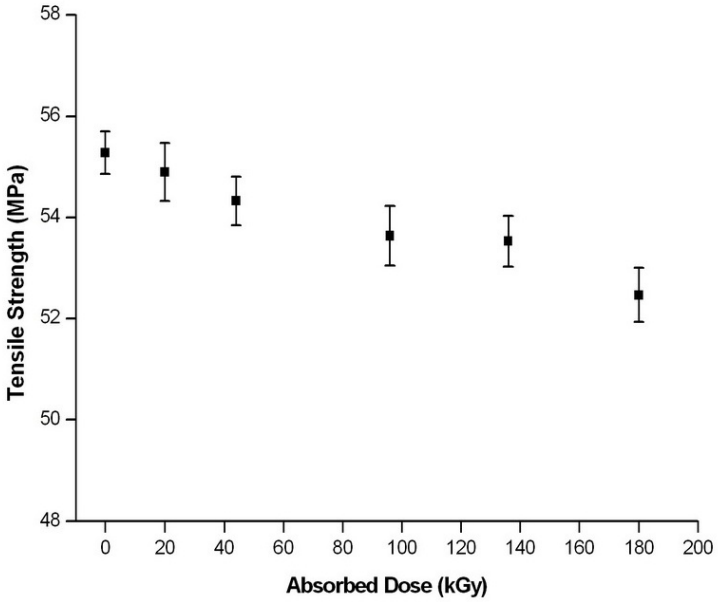

Figure 3.4 Effect of irradiation dose on tensile strength.

The information gathered from the literature suggests that polymers in which chain scission takes place (like polycarbonate) upon irradiation get weaker, their strength and modulus values decrease. In the tensile test results of this study presented above, a gradual decrease in the average tensile strength values with increasing dose is noticed. This is in accordance with the results of Golden et al. [19] and Arajuo et al. [25] where a decrease in the tensile strength took place with

increasing dose within the dose range applied in this study. No steady change in the average tensile modulus with increasing dose is observed. Although the graphs display the average values, large differences in the tensile modulus values of individual specimens at the same dose levels, together with the possible sources of error due to the physical conditions of the test specimens prevent strict deductions to be made from the obtained results.

3.2.2 Bending Tests

Representative flexural stress-strain curves from each specimen group are given in Figure 3.5.

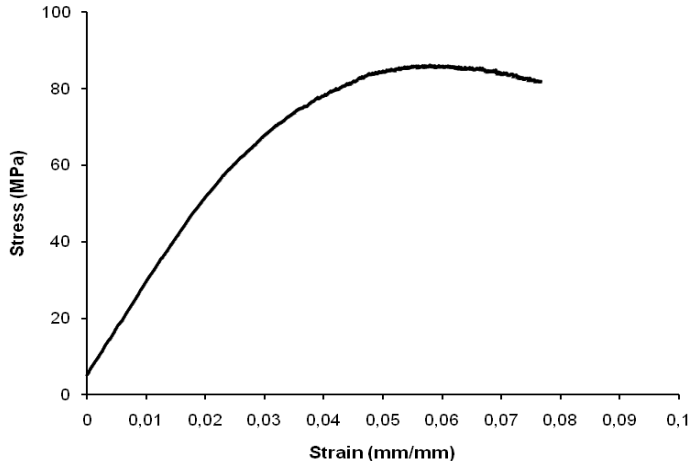

(a)

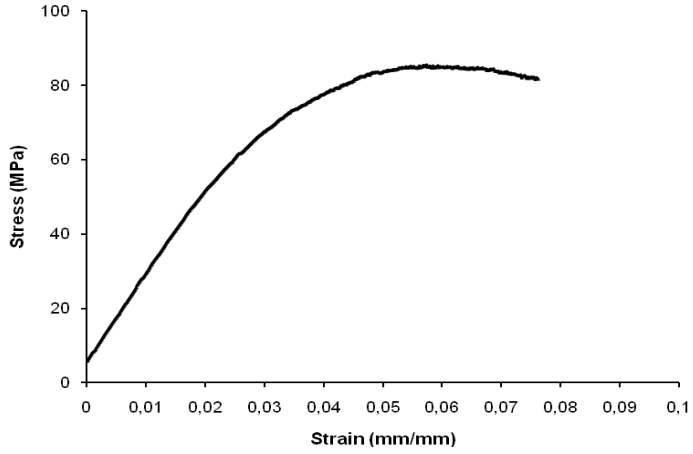

(b)

Figure 3.5 Representative flexural stress-strain curves of the specimens irradiated up to (a) 0, (b) 20, (c) 44, (d) 96, (e) 136, and (f) 180 kGy.

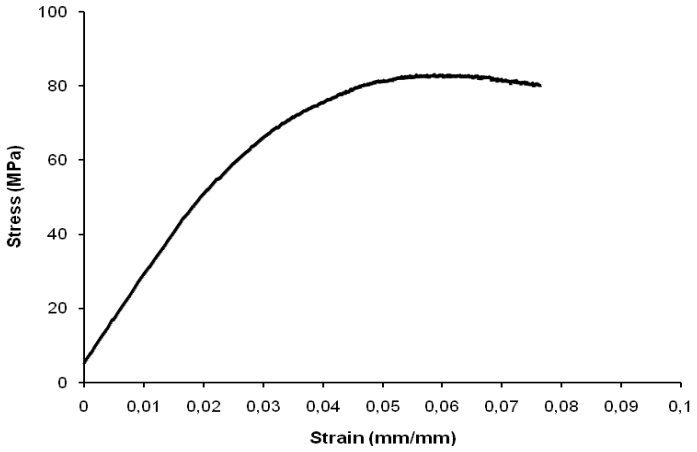

(c)

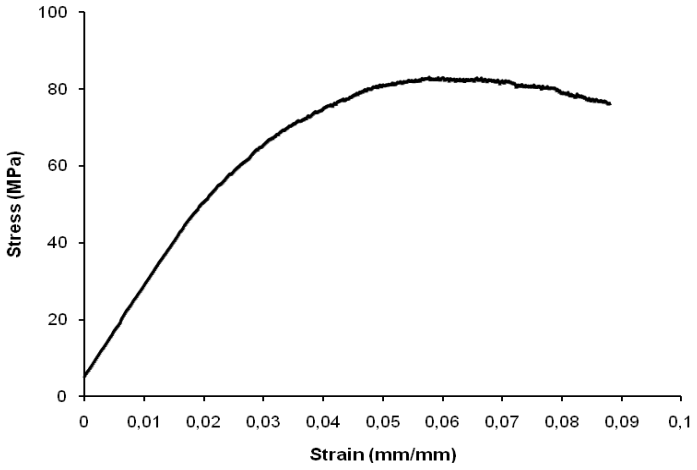

(d)

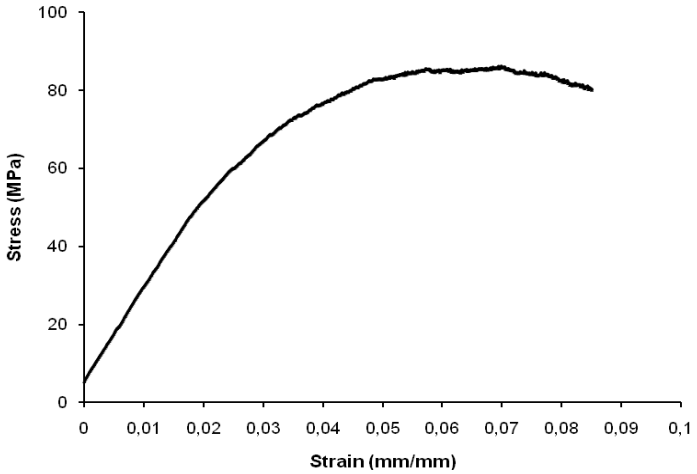

(e)

Figure 3.5 Representative flexural stress-strain curves of the specimens irradiated up to (a) 0, (b) 20, (c) 44, (d) 96, (e) 136, and (f) 180 kGy (cont'd).

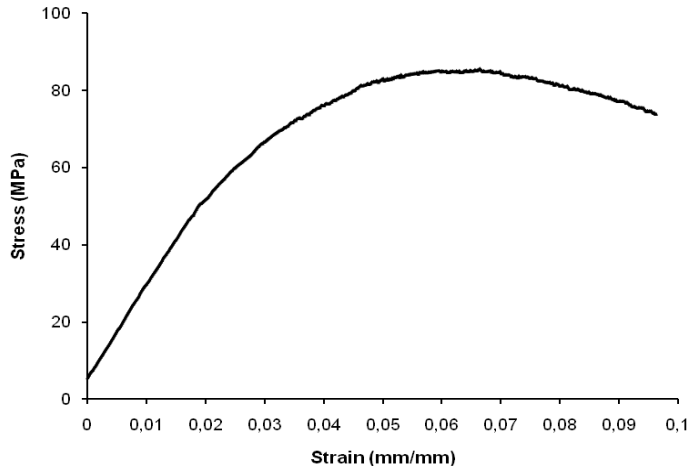

(f)

Figure 3.5 Representative flexural stress-strain curves of the specimens irradiated up to (a) 0, (b) 20, (c) 44, (d) 96, (e) 136, and (f) 180 kGy (cont'd).

The slope of the linear (elastic) portion on each curve was calculated and recorded as the flexural modulus value and the maximum stress attained on each curve was recorded as the flexural strength value. The values obtained from all specimens are given in Tables 3.3 and 3.4.

Table 3.3 Flexural modulus values of the test specimens

	Flexural Modulus (MPa)					
Absorbed Dose (kGy)	Specimen 1	Specimen 2	Specimen 3	Specimen 4	Specimen 5	Average
0	2427	2311	2385	2393	2350	2373 ± 45
20	2368	2307	2368	2365	2415	2365 ± 39
44	2382	2336	2384	2356	2372	2366 ± 20
96	2419	2364	2339	2353	2356	2366 ± 31
136	2390	2385	2358	2402	2380	2383 ± 16
180	2454	2411	2413	2435	2435	2429 ± 18

Table 3.4 Flexural strength values of the test specimens

	Flexural Strength (MPa)					
Absorbed Dose (kGy)	Specimen 1	Specimen 2	Specimen 3	Specimen 4	Specimen 5	Average
0	…	86,2	86,9	86,1	84,4	85,9 ± 1,1
20	85,2	84,8	85,5	83,8	86,7	85,2 ± 1,1
44	86,1	83,2	84,2	84,7	84,9	84,6 ± 1,1
96	85,0	85,5	83,2	83,1	85,5	84,4 ± 1,2
136	86,2	85,6	86,7	87,8	86,7	86,6 ± 0,8
180	87,9	85,6	85,8	86,3	87,3	86,6 ± 1,0

The effect of irradiation dose on the flexural modulus and the flexural strength are evaluated in Figures 3.6 and 3.7.

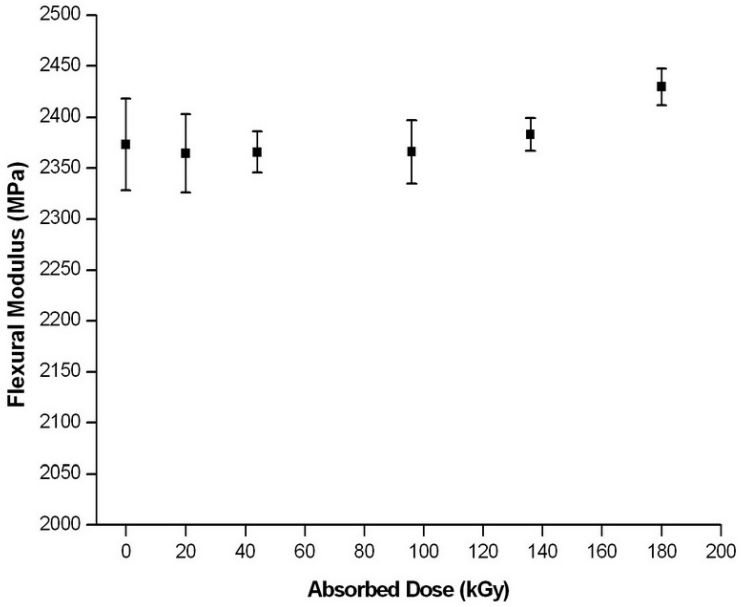

Figure 3.6 Effect of irradiation dose on the flexural modulus.

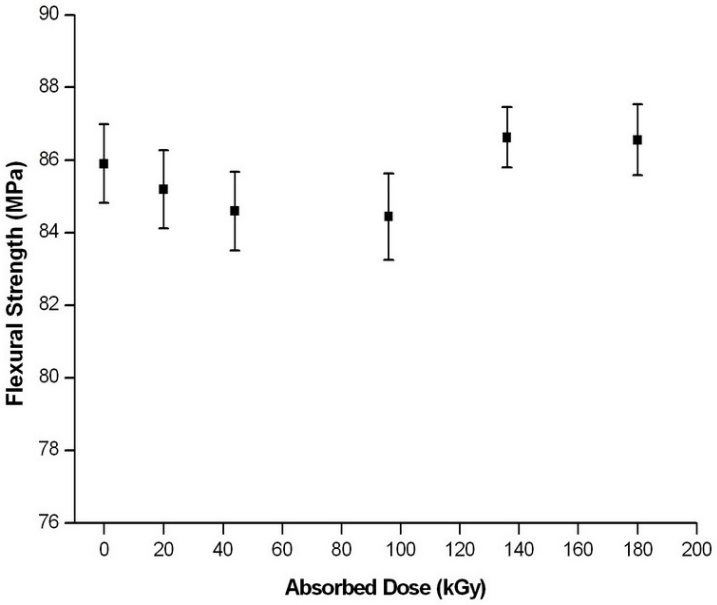

Figure 3.7 Effect of irradiation dose on the flexural strength.

The flexural modulus increased with increasing dose in the study of Golden et al. [19]. Likewise, the average flexural modulus values of the specimens irradiated at higher doses in this study are slightly higher than the flexural modulus value of the non-irradiated specimens. There is no steady change in the average flexural strength with increasing dose, this parameter decreases to a minimum at a dose of 96 kGy and then an increasing trend is observed.

3.2.3 Hardness Tests

The measured and recorded Shore D hardness values of the specimens are presented in Table 3.5.

Table 3.5 Shore D hardness values of the specimens

	Absorbed Dose of Specimen					
	0 kGy	20 kGy	44 kGy	96 kGy	136 kGy	180 kGy
Measurement 1	90	92	92	92	93	92
Measurement 2	91	92	92	92	92	92
Measurement 3	92	92	92	92	92	92
Measurement 4	92	92	92	92	92	92
Measurement 5	92	92	92	92	92	92
Measurement 6	91	92	92	92	92	92
Measurement 7	91	92	92	92	92	92
Average	91	92	92	92	92	92

Figure 3.8 shows that irradiation had almost no influence on the Shore D hardness of polycarbonate within the dose range studied.

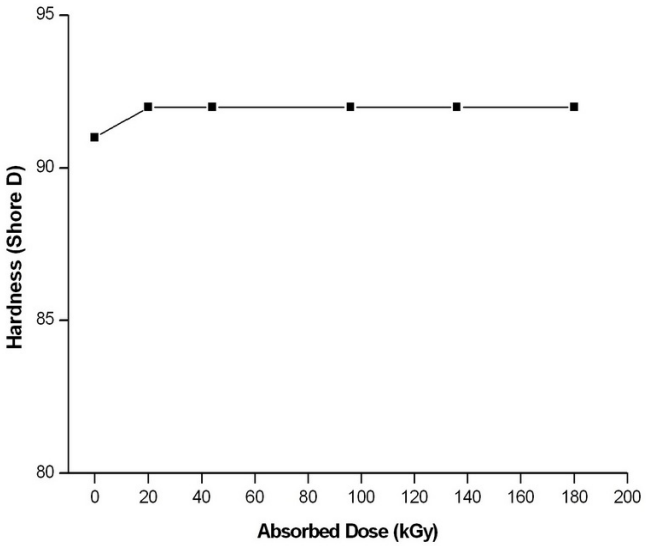

Figure 3.8 Effect of irradiation dose on the Shore D hardness.

3.3 Effects on the Molecular Weight

3.3.1 Dilute Solution Viscometry

In the dilute solution viscometric study, the mean efflux time t_0 of THF in the viscometer was determined as 141,39 s. Then, 15 ml of 0,5 g/dl solutions of

polymer samples irradiated at each dose was prepared, their efflux times were measured (4 times for each solution), and this procedure was repeated by diluting each solution by 4 ml three times. The measured efflux times of each solution and the calculated viscosity parameters (namely the relative viscosity η_r, the specific viscosity η_{sp}, the reduced viscosity η_{red}, and the inherent viscosity η_{inh}) at each condition are presented in Table 3.6.

Table 3.6 Viscosity parameters of solutions of specimens at each irradiation dose

0 kGy (non-irradiated) PC solution						
V (ml)	c (g/dl)	t (s)	η_r (t/t_0)	η_{sp} (η_r - 1)	η_{red} (η_{sp}/c)	η_{inh} (ln η_r)/c
15	0,5	179,92	1,2725	0,2725	0,5449	0,4819
19	0,3947	171,76	1,2148	0,2148	0,5441	0,4929
23	0,3261	167,02	1,1812	0,1812	0,5558	0,5108
27	0,2778	163,51	1,1564	0,1564	0,5632	0,5232

20 kGy irradiated PC solution						
V (ml)	c (g/dl)	t (s)	η_r (t/t_0)	η_{sp} (η_r - 1)	η_{red} (η_{sp}/c)	η_{inh} (ln η_r)/c
15	0,5	179,59	1,2702	0,2702	0,5403	0,4783
19	0,3947	170,41	1,2052	0,2052	0,5200	0,4730
23	0,3261	165,72	1,1720	0,1720	0,5276	0,4868
27	0,2778	162,94	1,1524	0,1524	0,5486	0,5106

44 kGy irradiated PC solution						
V (ml)	c (g/dl)	t (s)	η_r (t/t_0)	η_{sp} (η_r - 1)	η_{red} (η_{sp}/c)	η_{inh} (ln η_r)/c
15	0,5	182,81	1,2929	0,2929	0,5859	0,5138
19	0,3947	174,75	1,2360	0,2360	0,5978	0,5367
23	0,3261	168,01	1,1883	0,1883	0,5773	0,5289
27	0,2778	163,82	1,1586	0,1586	0,5710	0,5300

96 kGy irradiated PC solution						
V (ml)	c (g/dl)	t (s)	η_r (t/t_0)	η_{sp} (η_r - 1)	η_{red} (η_{sp}/c)	η_{inh} (ln η_r)/c
15	0,5	181,49	1,2836	0,2836	0,5673	0,4994
19	0,3947	173,32	1,2258	0,2258	0,5721	0,5158
23	0,3261	164,60	1,1642	0,1642	0,5034	0,4661
27	0,2778	163,88	1,1590	0,1590	0,5725	0,5313

Table 3.6 Viscosity parameters of solutions of specimens at each irradiation dose (cont'd)

136 kGy irradiated PC solution						
V (ml)	c (g/dl)	t (s)	η_r (t/t_0)	η_{sp} (η_r - 1)	η_{red} (η_{sp}/c)	η_{inh} (ln η_r)/c
15	0,5	177,96	1,2586	0,2586	0,5172	0,4600
19	0,3947	173,28	1,2256	0,2256	0,5715	0,5153
23	0,3261	168,26	1,1900	0,1900	0,5827	0,5335
27	0,2778	164,13	1,1609	0,1609	0,5790	0,5369

180 kGy irradiated PC solution						
V (ml)	c (g/dl)	t (s)	η_r (t/t_0)	η_{sp} (η_r - 1)	η_{red} (η_{sp}/c)	η_{inh} (ln η_r)/c
15	0,5	180,33	1,2754	0,2754	0,5507	0,4865
19	0,3947	174,41	1,2335	0,2335	0,5916	0,5317
23	0,3261	171,42	1,2124	0,2124	0,6513	0,5906
27	0,2778	164,55	1,1638	0,1638	0,5895	0,5459

The intrinsic viscosities of the solutions of each specimen group were determined by plotting the inherent viscosity versus concentration graphs and extrapolating to c=0 as illustrated in Figure 3.9.

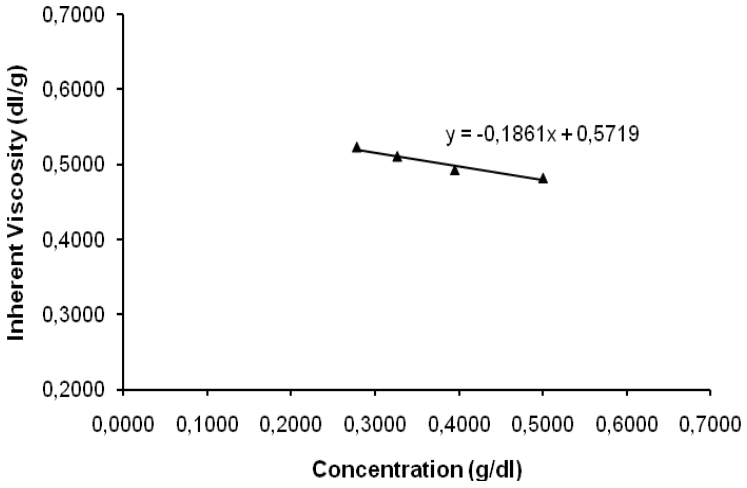

(a)

Figure 3.9 Inherent viscosity versus concentration plots of the solutions of the specimens with irradiation doses of (a) 0, (b) 20, (c) 44, (d) 96, (e) 136, and (f) 180 kGy.

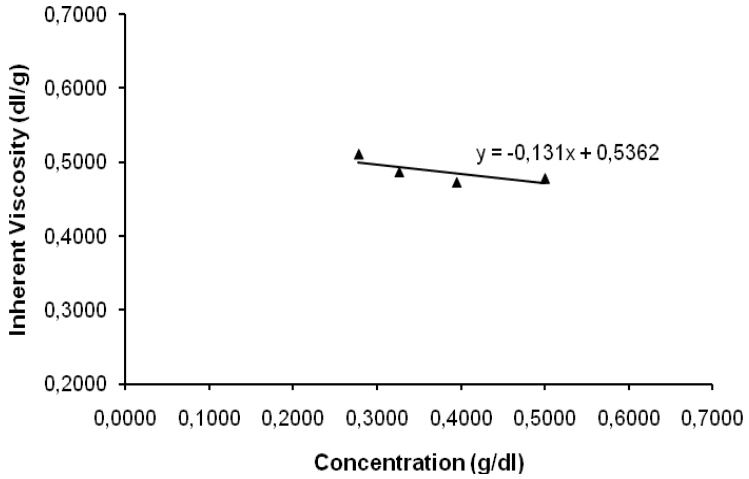

(b)

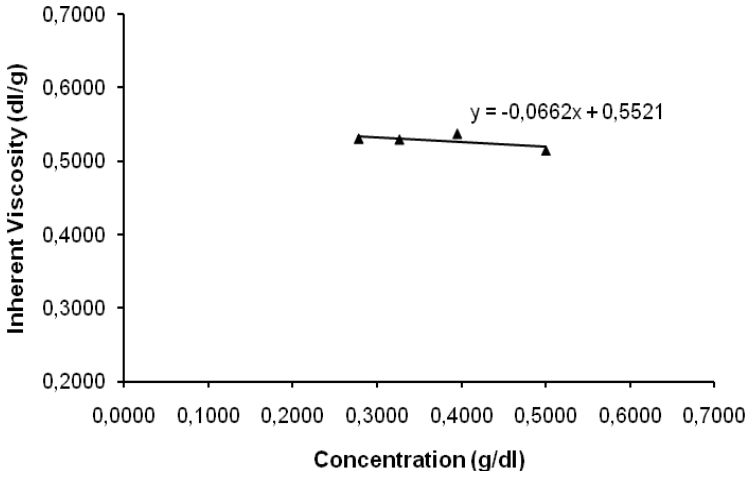

(c)

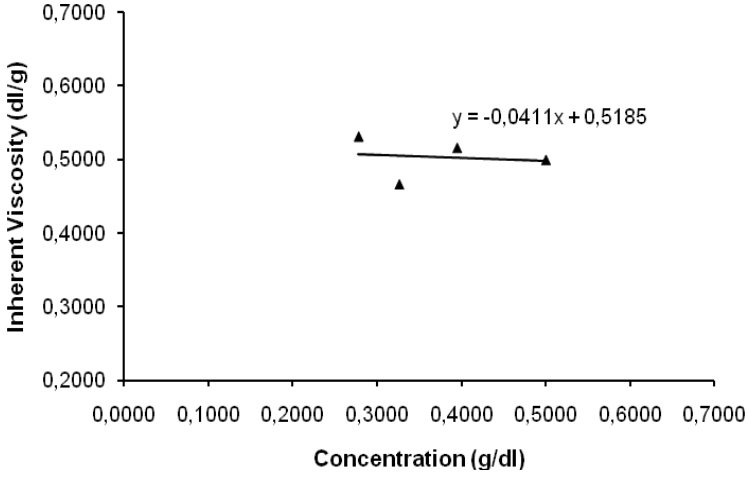

(d)

Figure 3.9 Inherent viscosity versus concentration plots of the solutions of the specimens with irradiation doses of (a) 0, (b) 20, (c) 44, (d) 96, (e) 136, and (f) 180 kGy (cont'd).

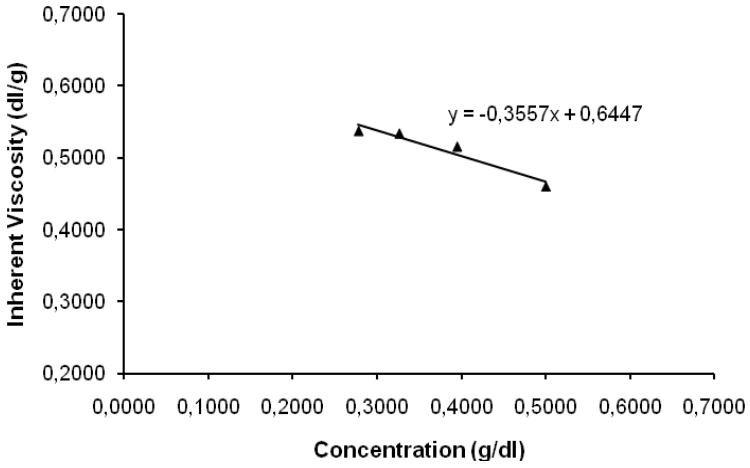

(e)

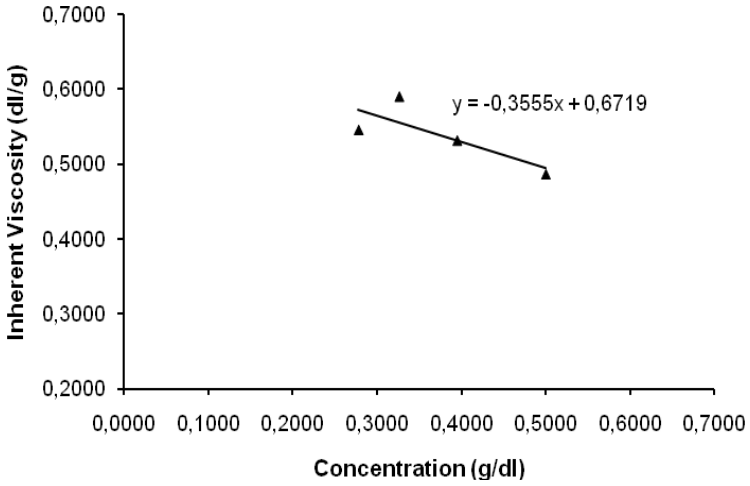

(f)

Figure 3.9 Inherent viscosity versus concentration plots of the solutions of the specimens with irradiation doses of (a) 0, (b) 20, (c) 44, (d) 96, (e) 136, and (f) 180 kGy (cont'd).

As mentioned in the previous chapter, once the intrinsic viscosity is determined and the constants K and a are known, the viscosity average molecular weight (M_v) of a polymer dissolved in a solvent can be calculated from the Mark-Houwink equation:

$$[\eta] = K (M_v)^a \qquad (3.1)$$

For the polycarbonate solutions in THF at 25 °C, the Mark-Houwink constants K and a are reported in the literature as 38,9 × 10^{-3} ml/g and 0,70 respectively [48].

The intrinsic viscosity values and the corresponding viscosity average molecular weights calculated for each specimen are given in Table 3.7 and evaluated in Figure 3.10.

Table 3.7 Intrinsic viscosities of solutions and the corresponding molecular weights of specimens

Absorbed Dose (kGy)	[η] (dl/g)	M_v
0	0,5719	33482,3
20	0,5362	30536,9
44	0,5521	31838,6
96	0,5185	29107,1
136	0,6447	39733,3
180	0,6719	42149,5

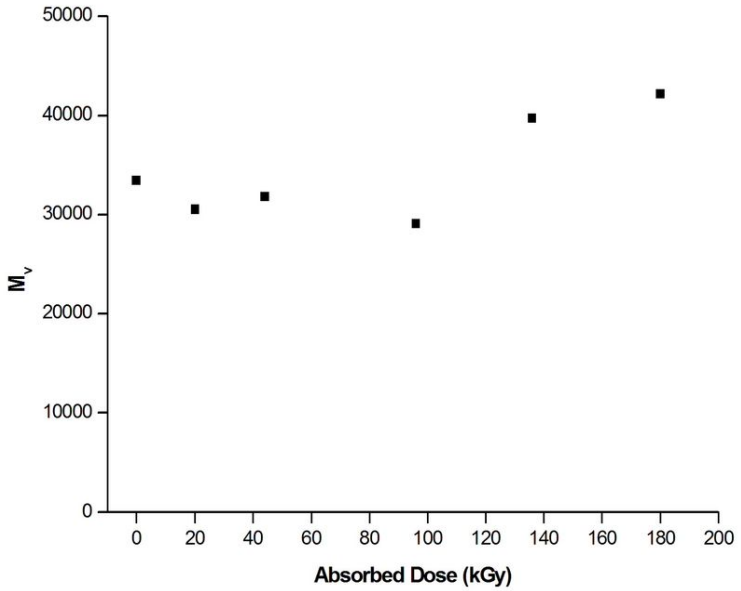

Figure 3.10 Effect of irradiation dose on the M_v of the specimens.

The viscosity average molecular weight M_v is observed to decrease slightly up to an absorbed dose of 96 kGy and then increase with increasing dose, reaching its maximum value at the highest dose applied in this study, which is 180 kGy. Before commenting on the effect of irradiation dose on the molecular weight, it

was preferred to determine the other molecular weight averages (M_n, M_w and M_z) by gel permeation chromatography.

3.3.2 Gel Permeation Chromatography

Three groups of specimens having irradiation doses of 0, 96 and 180 kGy were subjected to molecular weight determination by gel permeation chromatography (GPC). Table 3.8 shows the results obtained.

Table 3.8 Molecular weights of the three groups of specimens determined by GPC

Absorbed Dose (kGy)	M_n	M_w	M_z	Dispersity
0	30630	90012	175354	2,93863
96	12308	33154	64473	2,69374
180	14047	39853	79351	2,83704

Then, effect of the irradiation dose on the number average molecular weight (M_n), the weight average molecular weight (M_w) and the size average molecular weight (M_z) of the specimens are displayed graphically in Figure 3.11.

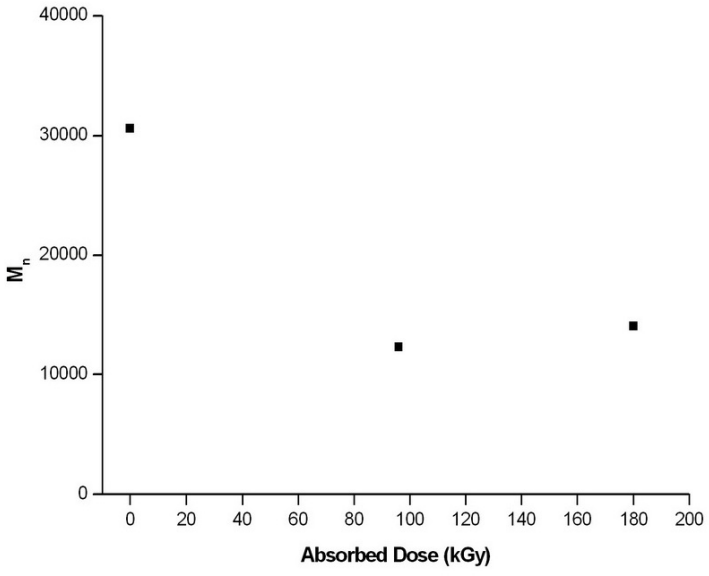

(a)

Figure 3.11 Effect of irradiation dose on the (a) M_n, (b) M_w, and (c) M_z of the three groups of specimens.

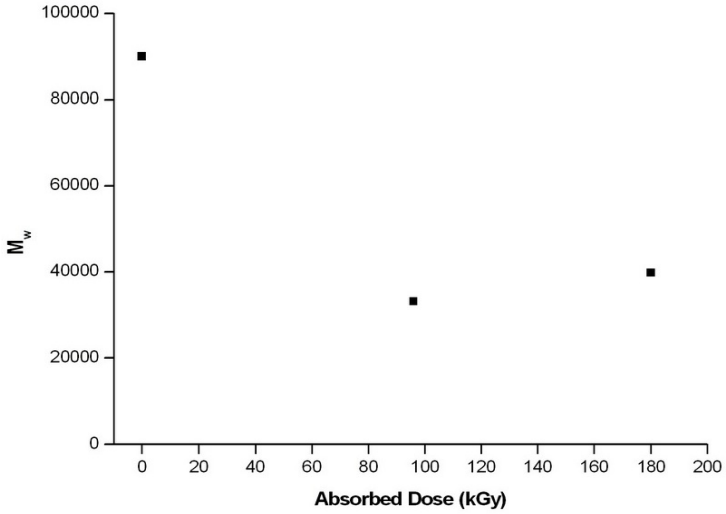

(b)

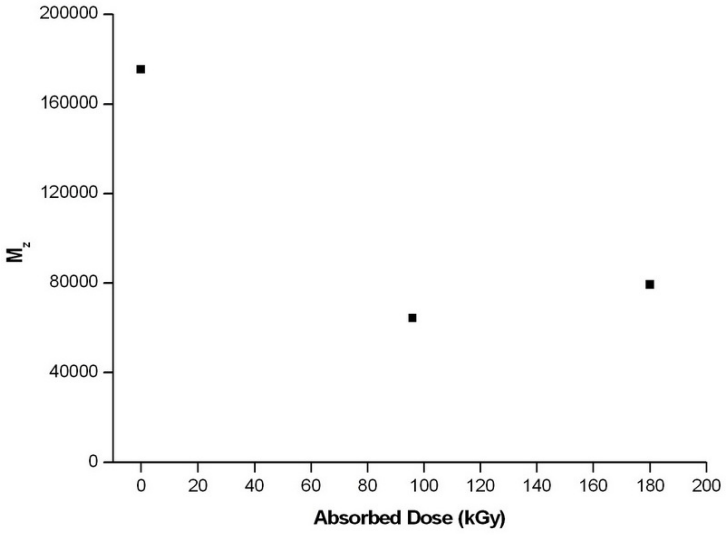

(c)

Figure 3.11 Effect of irradiation dose on the (a) M_n, (b) M_w, and (c) M_z of the three groups of specimens (cont'd).

Taking a look at the variation of M_n, M_w and M_z with absorbed dose (Figure 3.11), again a decrease until a dose of 96 kGy and then an increase up to 180 kGy in the molecular weight is noticed. As stated in the literature, the decrease in the molecular weight can be attributed to chain scission. There are two occasions in the studies mentioned in the previous chapter where an increase in the intrinsic viscosity (which may be regarded as an increase in the molecular weight) took place upon irradiation of polycarbonate specimens. In the studies of Acierno et al. [23] and Arajuo et al. [25], the intrinsic viscosity rose to a maximum value at a

dose around 40 kGy and then decreased. Acierno et al. considered this increase in molecular weight at low doses as just a simple branching, not a significant crosslinking. Although the viscosity average molecular weight increased to its highest value at 180 kGy in our study and this value does not match the peak value of these authors, a similarity is present in the sense that there is a region where the molecular weight increases with increasing amount of absorbed dose.

3.4 Effects on the Molecular Structure

3.4.1 Infrared Spectroscopy

The ATR-FTIR spectra of the specimens of this study are given in Figure 3.12. No remarkable change is present on the spectra of the specimens irradiated up to 96 kGy. The peak intensities on the spectrum of the 96 kGy irradiated specimen are significantly lowered, being in fact the lowermost among all spectra obtained. The lowest molecular weight values measured also belong to the specimen irradiated at this dose, which may be interpreted that the highest yield of chain scission in this study occurred at 96 kGy. Similar to the work of De Melo et al. [27], absorbance intensities of peaks at 1769 cm^{-1} and 767 cm^{-1} were measured and the oxidation indices were calculated. The oxidation index is defined as the ratio of the absorbance at 1769 cm^{-1} (corresponding to the C=O stretch band) to the absorbance at 767 cm^{-1} (corresponding to the out-of-plane bending absorption of the C–H bond on the aromatic rings). The results are given in Table 3.9 and a graphical representation can be seen Figure 3.13. In Figure 3.13, the oxidation index is seen to be decreasing with increasing dose, in accordance with the referred studies in the literature. This behavior can be considered as an indication that the carbonyl group is prone to the irradiation and the chain scission starts with the breakage of C=O bonds.

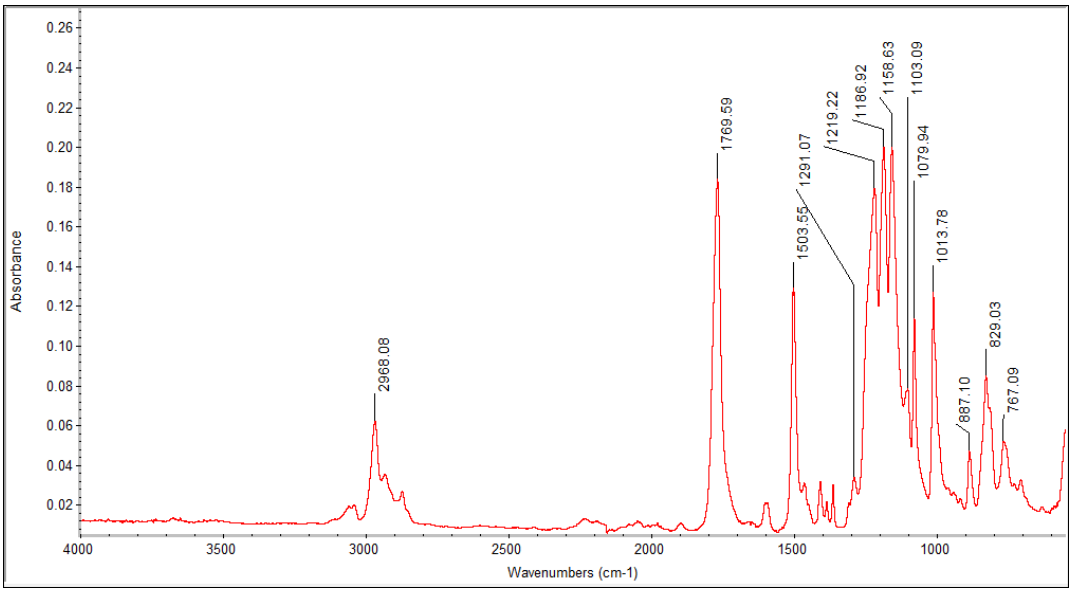

(a)

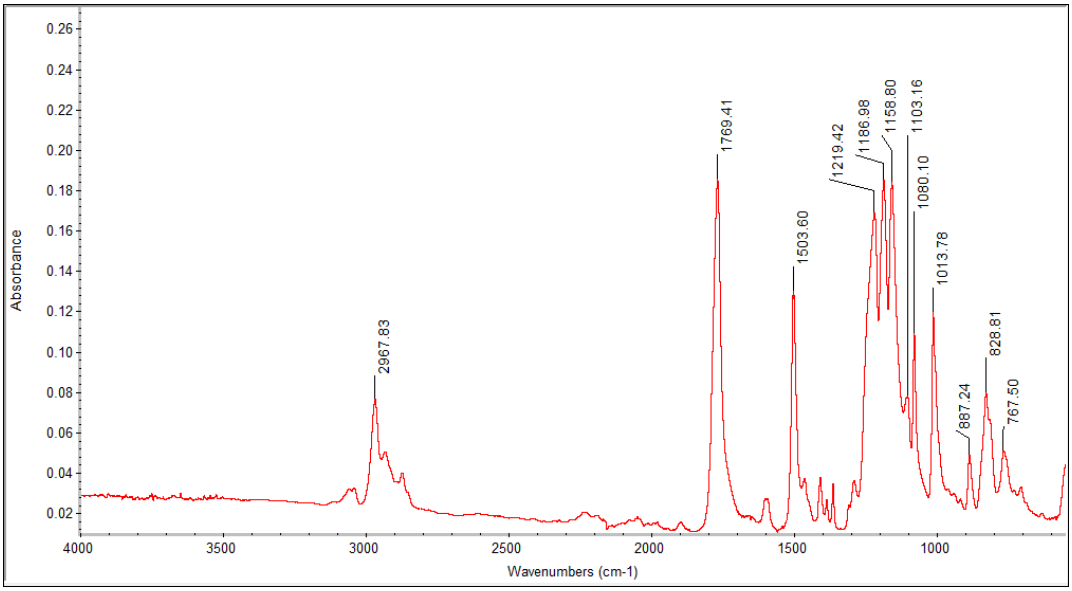

(b)

Figure 3.12 ATR-FTIR spectra of the specimens irradiated up to (a) 0, (b) 20, (c) 44, (d) 96, (e) 136, and (f) 180 kGy.

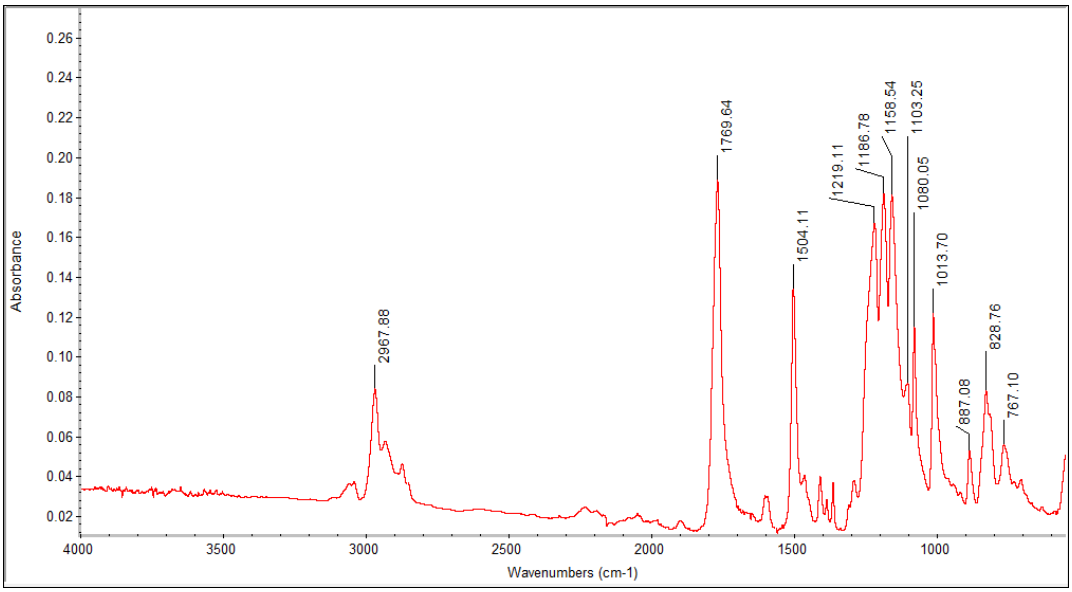

(c)

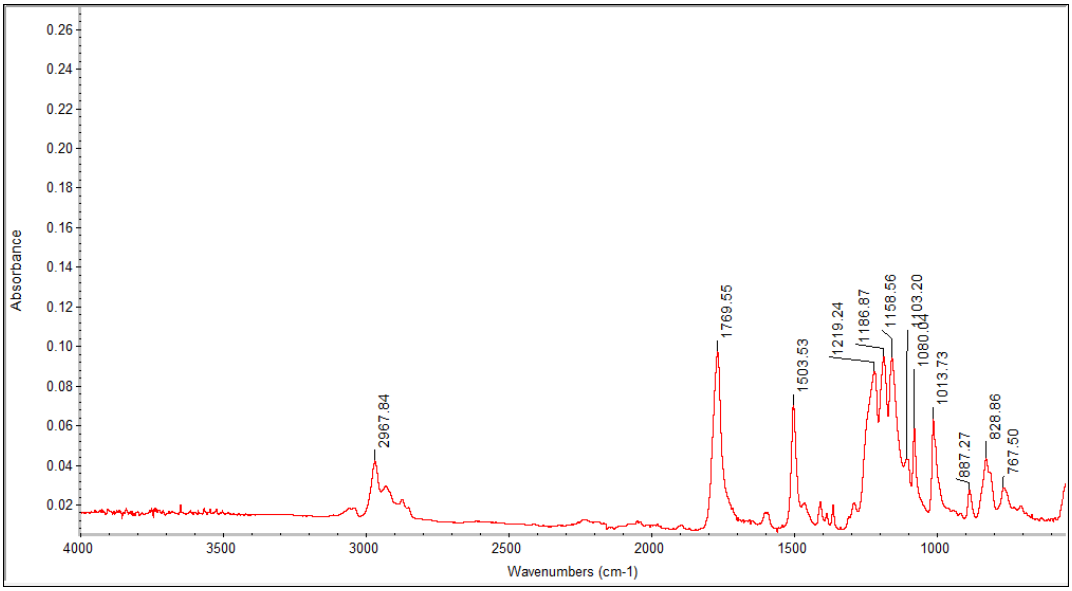

(d)

Figure 3.12 ATR-FTIR spectra of the specimens irradiated up to (a) 0, (b) 20, (c) 44, (d) 96, (e) 136, and (f) 180 kGy (cont'd).

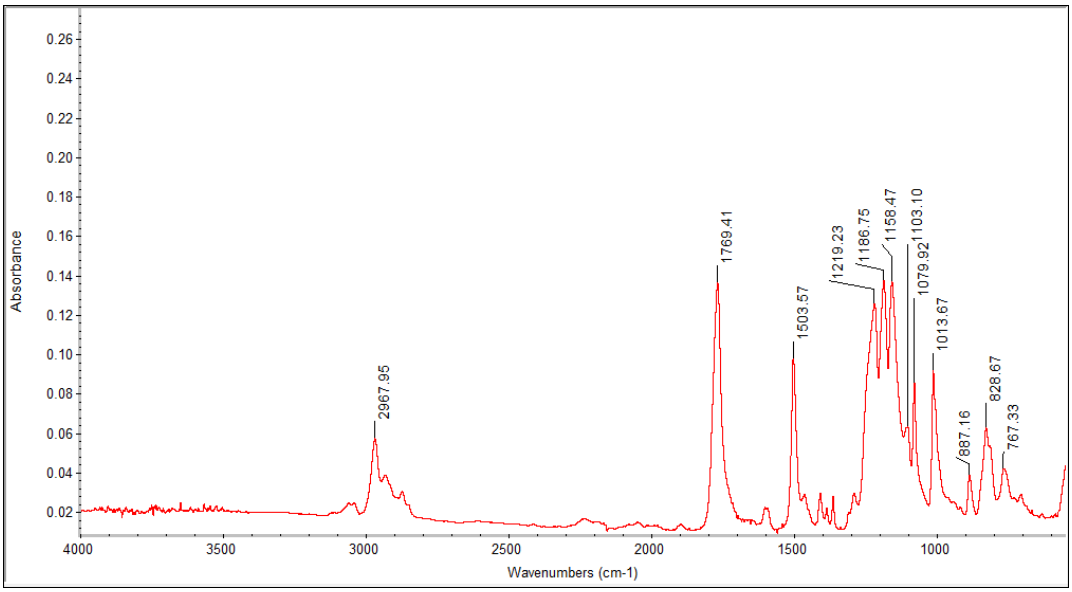

(e)

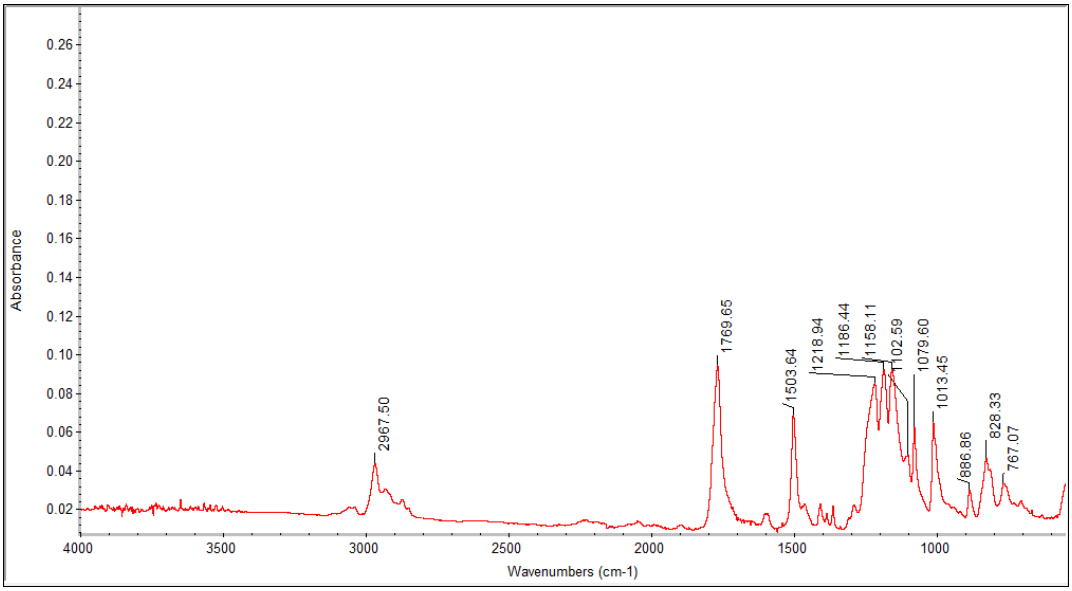

(f)

Figure 3.12 ATR-FTIR spectra of the specimens irradiated up to (a) 0, (b) 20, (c) 44, (d) 96, (e) 136, and (f) 180 kGy (cont'd).

Table 3.9 Absorbance intensities at 1769 cm^{-1}, 767 cm^{-1} and oxidation indices at each dose

Dose (kGy)	Absorbance at 1769 cm^{-1}	Absorbance at 767 cm^{-1}	Oxidation Index
0	0,182	0,052	3,500
20	0,182	0,052	3,500
44	0,184	0,058	3,172
96	0,096	0,030	3,200
136	0,136	0,044	3,091
180	0,096	0,034	2,824

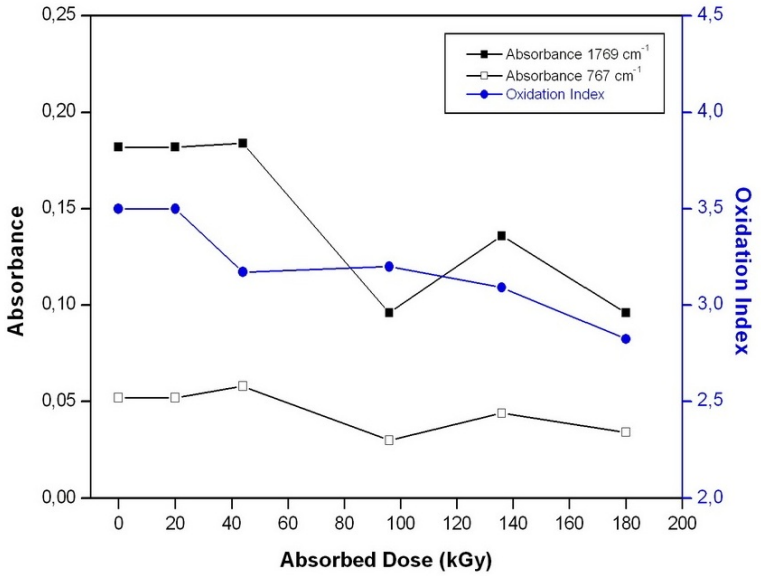

Figure 3.13 Absorbances in characteristic bands and oxidation index values versus irradiation dose.

3.4.2 Nuclear Magnetic Resonance Spectroscopy

Three groups of specimens having irradiation doses of 0, 96 and 180 kGy were subjected to nuclear magnetic resonance (NMR) spectroscopy. The ^{1}H and ^{13}C NMR spectra of the non-irradiated, 96 kGy irradiated and the 180 kGy irradiated specimens are presented in Figures 3.14 and 3.15. Almost no changes in the resonances were observed, only the peak shift values increased a little with increasing dose and slight differences between the splitting patterns of some peaks appeared. This is in accordance with the results of Babanalbandi et al. [21], where no detectable changes appeared in the ^{13}C NMR spectrum of

polycarbonate irradiated up to 4 and 10 MGy at ambient temperature. These unaffected NMR spectra could be interpreted that the molecular weight increase observed between 96 kGy and 180 kGy irradiated specimens can hardly be attributed to crosslinking.

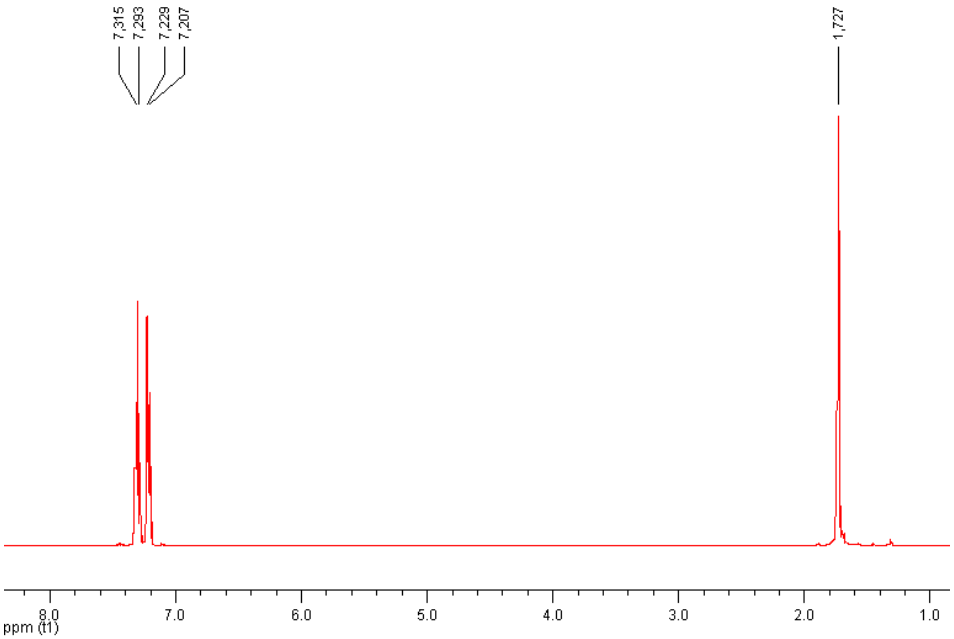

(a)

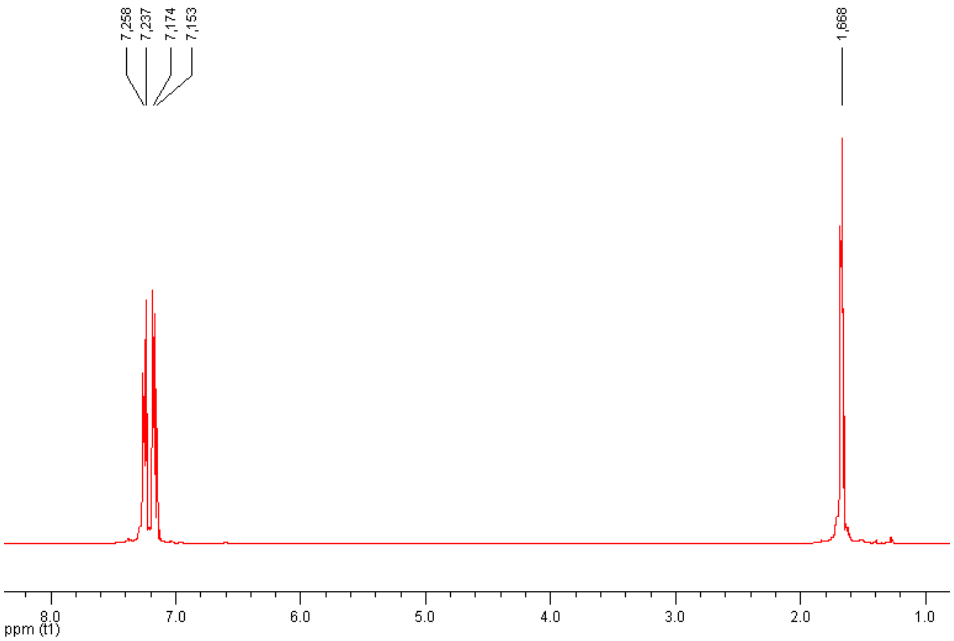

(b)

Figure 3.14 ^{1}H NMR spectra of the specimens irradiated up to (a) 0, (b) 96, and (c) 180 kGy.

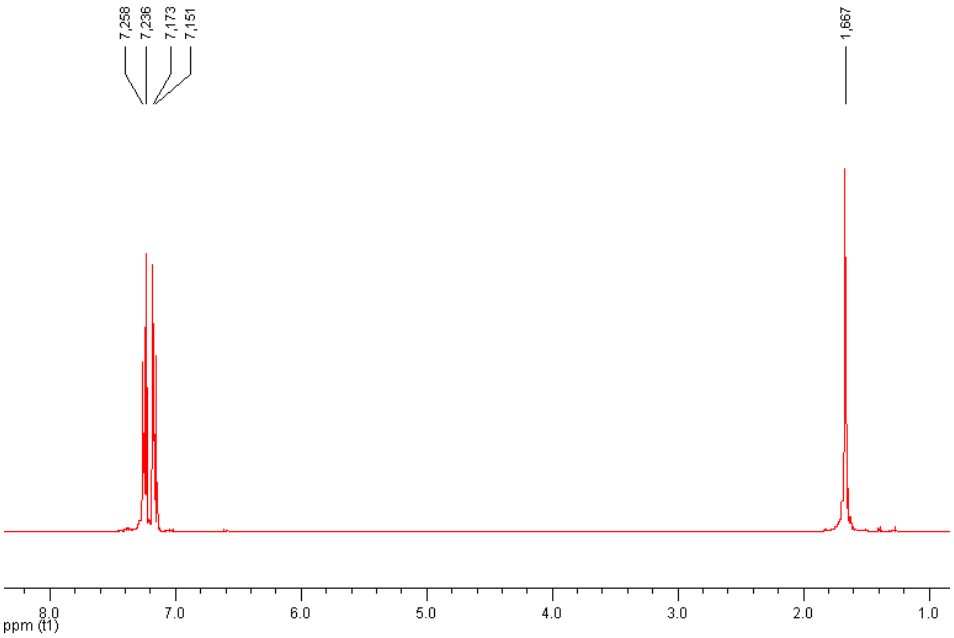

(c)

Figure 3.14 ^{1}H NMR spectra of the specimens irradiated up to (a) 0, (b) 96, and (c) 180 kGy (cont'd).

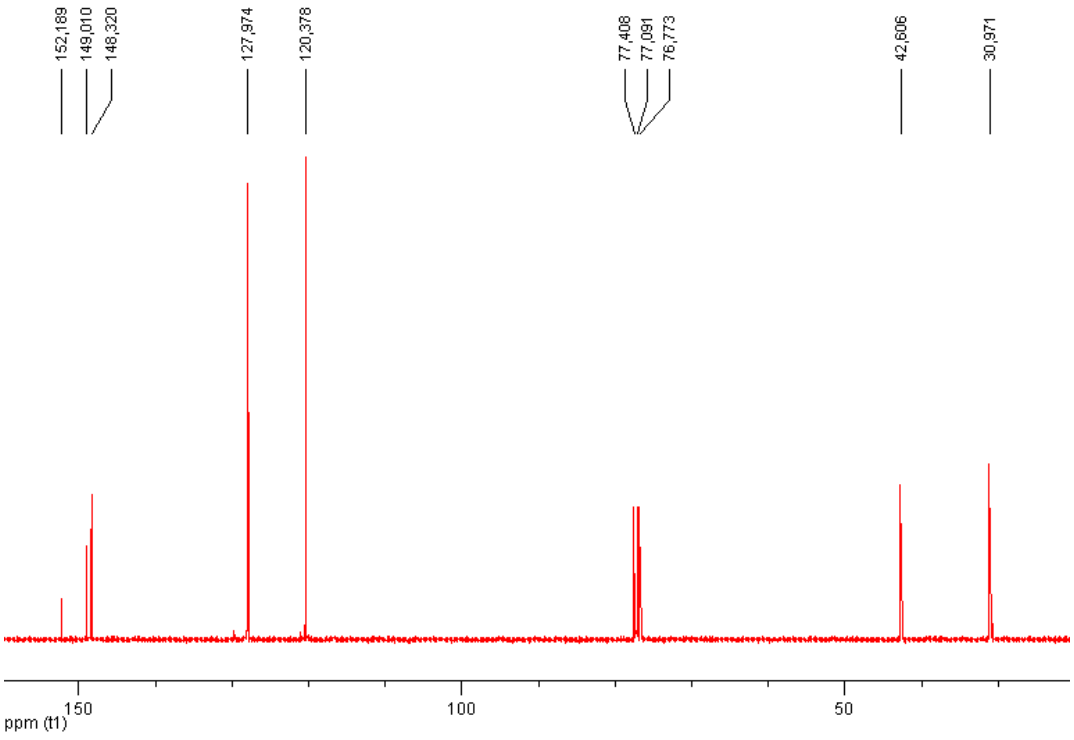

(a)

Figure 3.15 ^{13}C NMR spectra of the specimens irradiated up to (a) 0, (b) 96, and (c) 180 kGy.

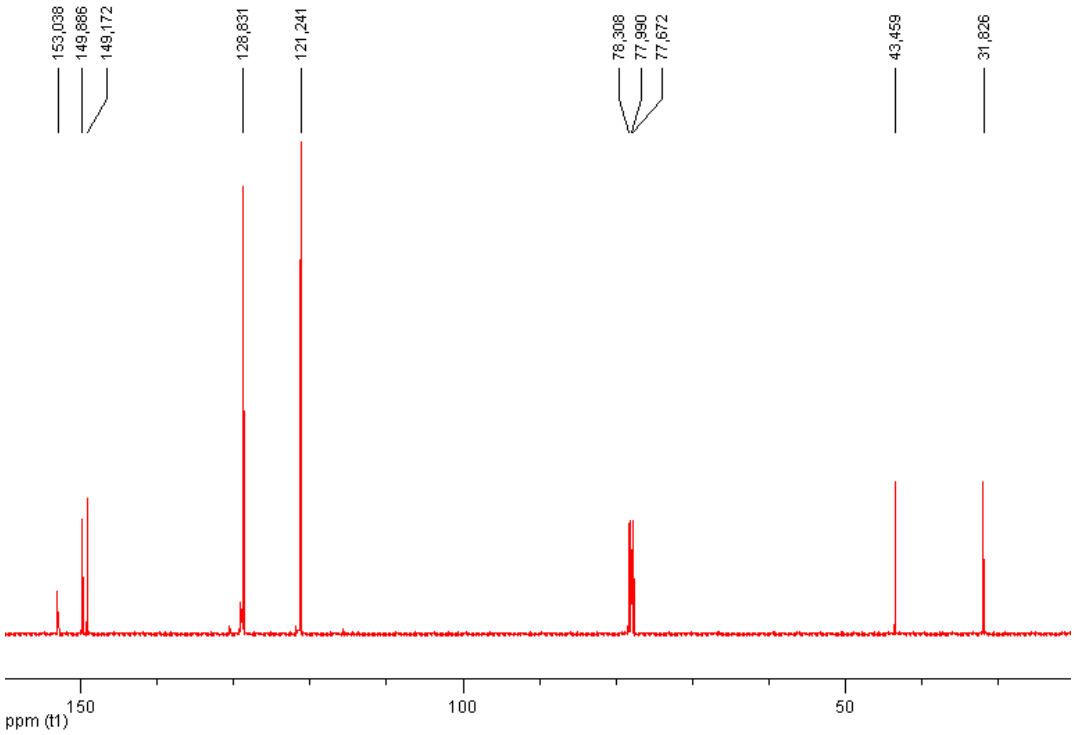

(b)

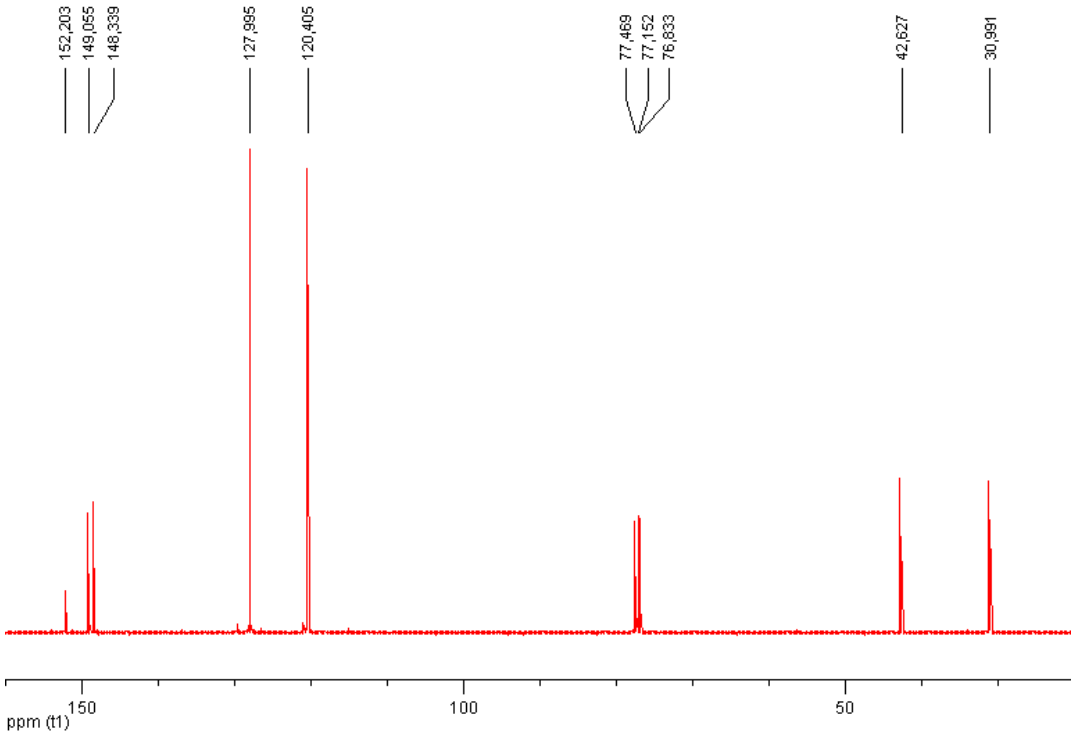

(c)

Figure 3.15 ^{13}C NMR spectra of the specimens irradiated up to (a) 0, (b) 96, and (c) 180 kGy (cont'd).

3.5 Effects on the Thermal Behavior

3.5.1 Differential Scanning Calorimetry

Differential scanning calorimetry (DSC) curves obtained for the specimens are given in Figure 3.16. The glass transition temperatures marked on the curves are tabulated in Table 3.10 and the effect of irradiation dose is evaluated in Figure 3.17.

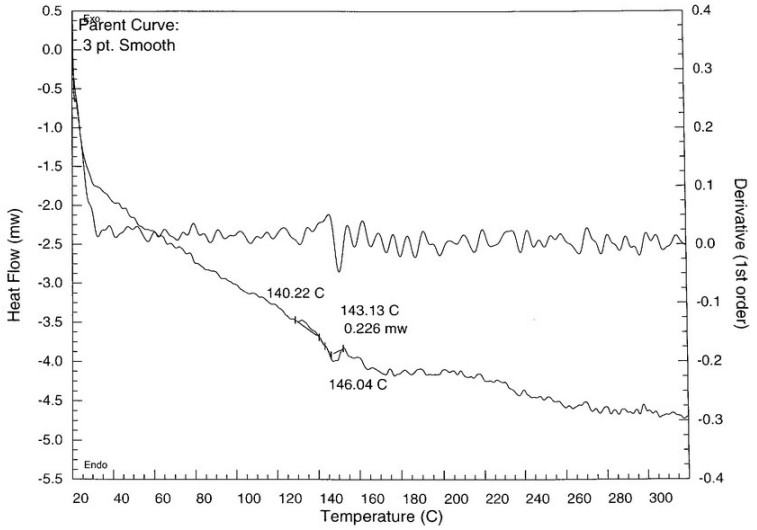

(a)

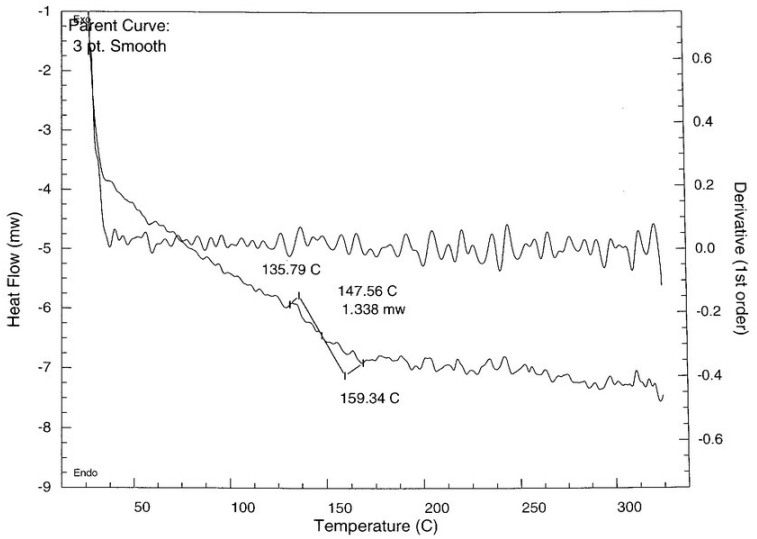

(b)

Figure 3.16 DSC curves of the specimens irradiated up to (a) 0, (b) 20, (c) 44, (d) 96, (e) 136, and (f) 180 kGy.

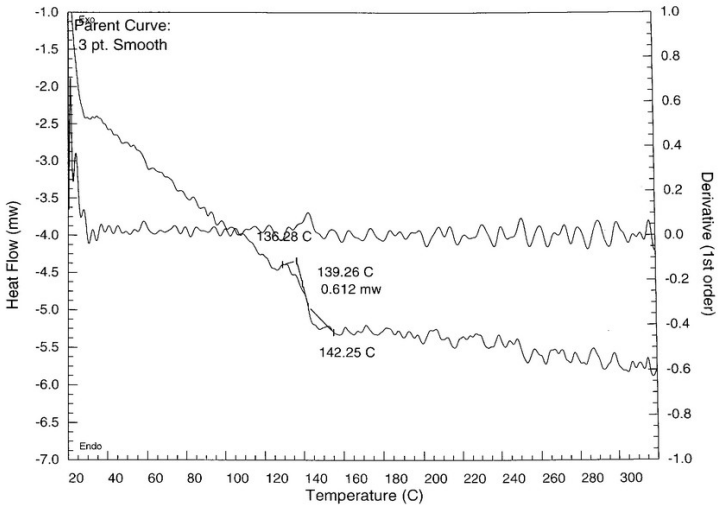

(c)

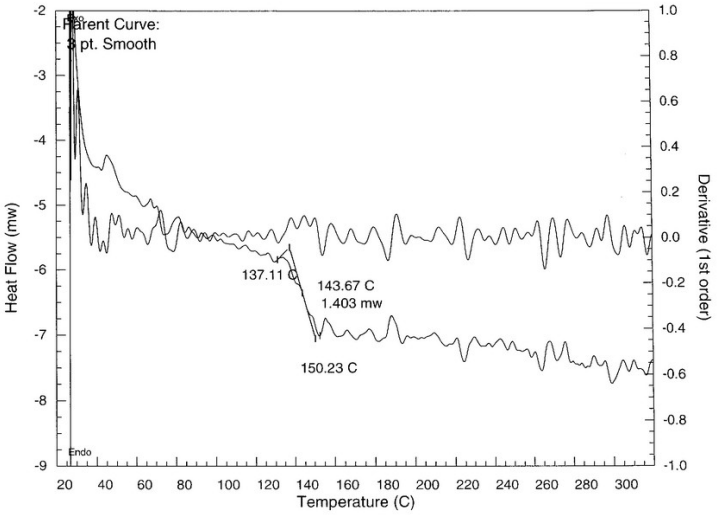

(d)

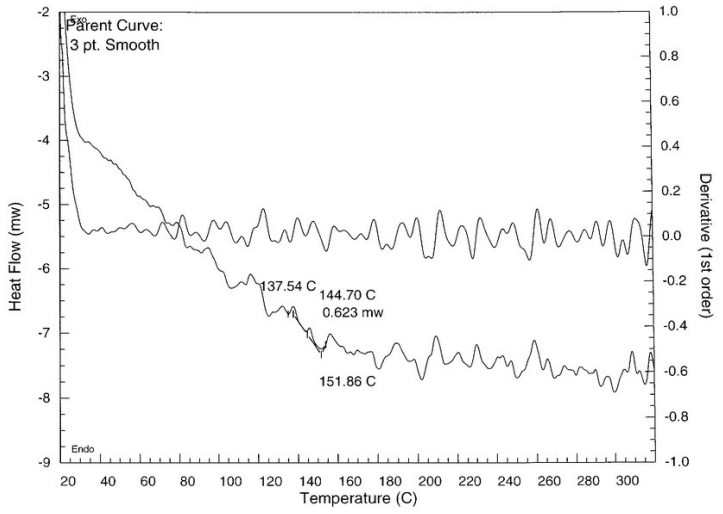

(e)

Figure 3.16 DSC curves of the specimens irradiated up to (a) 0, (b) 20, (c) 44, (d) 96, (e) 136, and (f) 180 kGy (cont'd).

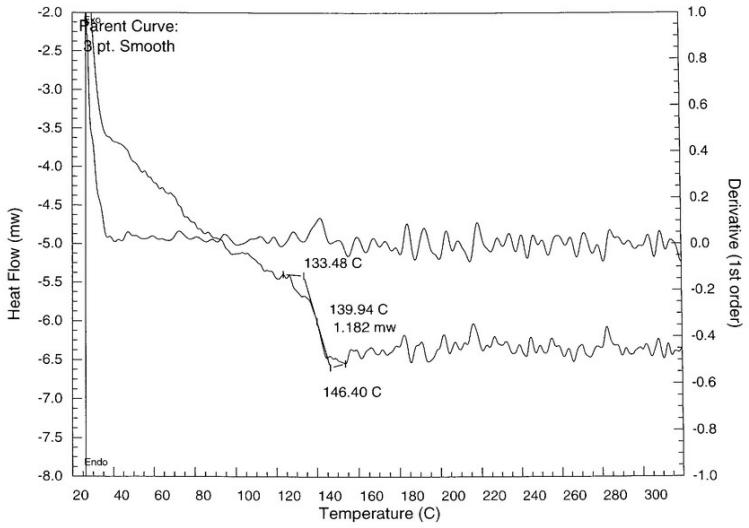

(f)

Figure 3.16 DSC curves of the specimens irradiated up to (a) 0, (b) 20, (c) 44, (d) 96, (e) 136, and (f) 180 kGy (cont'd).

Table 3.10 T_g values obtained from DSC curves of the specimens

Absorbed Dose (kGy)	T_g (°C)
0	143,13
20	147,56
44	139,26
96	143,67
136	144,70
180	139,94

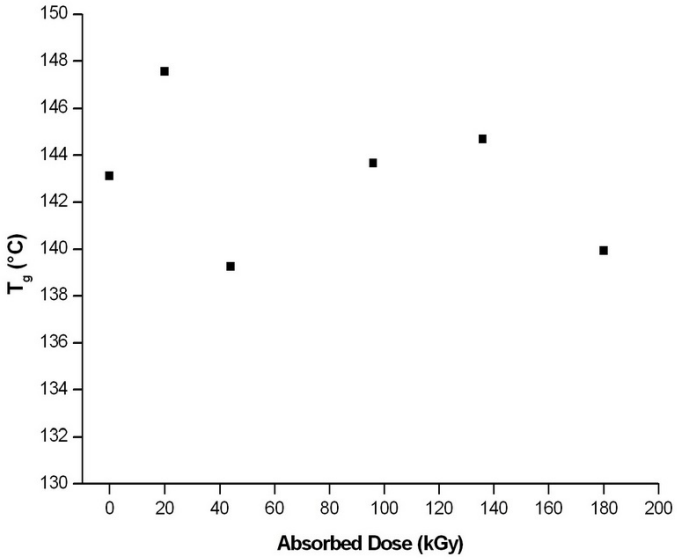

Figure 3.17 Effect of irradiation dose on the T_g values of the specimens.

The DSC curves (heat flow versus temperature) seem to be steeper up to the glass transition temperatures, indicating that the amount of heat required to keep the temperature equal to the reference in these regions are higher than those after the transitions. In the studies of Kalkar et al. [24] and Sinha et al. [28] very clear decreases in T_g were observed as the absorbed dose of the specimens increased. The reason for the decrease in T_g with an increase in absorbed dose was claimed as the increase in excess volume and chain mobility due to scissioning of the chains under the effect of irradiation. Below T_g no segmental motion of the molecules exists, so parts of the molecule can not wiggle around but only make slight vibrations. At T_g, segmental motion of the molecules starts. The molecular chains are scissioned by the irradiation and this causes the average chain length to decrease. The mobility of the chains is enhanced by the decrease in polymer chain length, and as a result, the glass transition temperature (T_g) of the polymer decreases. In this study only at some dose levels, especially at the maximum dose, the T_g turned out to be lower than that of the non-irradiated specimen. However, it should be kept in mind that the maximum dose in this study was much lower than those in the referred studies. The T_g of the specimen irradiated at maximum dose in this study (180 kGy) is lower than that of the non-irradiated specimen by 3-4 °C. In the work of Sinha et al. [28] a dose of 10^6 Gy (1000 kGy) was needed to observe a decrease of 9-10 °C in T_g.

3.5.2 Dynamic Mechanical Analysis

Dynamic mechanical analysis (DMA) curves of the specimens in this study are given in Figure 3.18. On each graph, the variation of *E'*, *E"* and tanδ with temperature are displayed. In the glassy region, the material exhibits mainly elastic behavior and energy loss by means of heat is low. For this reason, the storage modulus (*E'*) is high in this region. Upon being converted into a rubbery state at the glass transition, the stiffness decreases and more energy is lost as heat. So, the glass transition results in a decrease in the storage modulus (*E'*) and an increase in the loss modulus (*E"*). This is exactly what has been observed on the curves in Figure 3.18. Both the loss modulus (*E"*) and the dissipation factor (tanδ, the ratio of the loss modulus to the storage modulus) go through a maximum at the glass transition. The temperatures corresponding to the peak

values of tanδ, which are assigned as the glass transition temperatures determined by DMA, are tabulated in Table 3.11 and the effect of irradiation dose on these temperatures are evaluated in Figure 3.19.

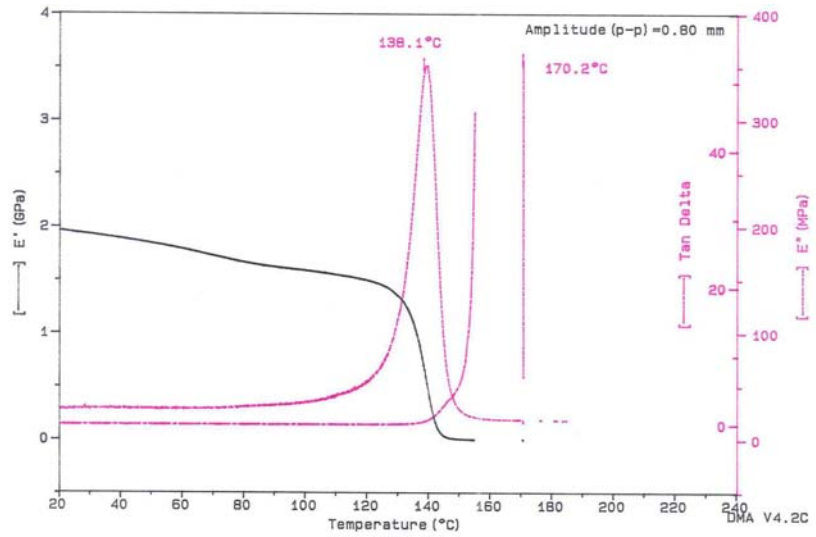

(a)

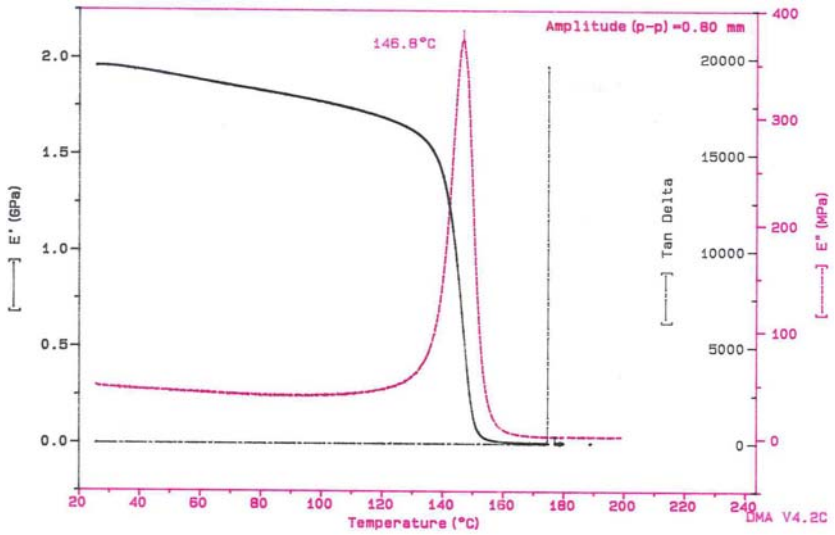

(b)

Figure 3.18 DMA curves of the specimens irradiated up to (a) 0, (b) 20, (c) 44, (d) 96, (e) 136, and (f) 180 kGy.

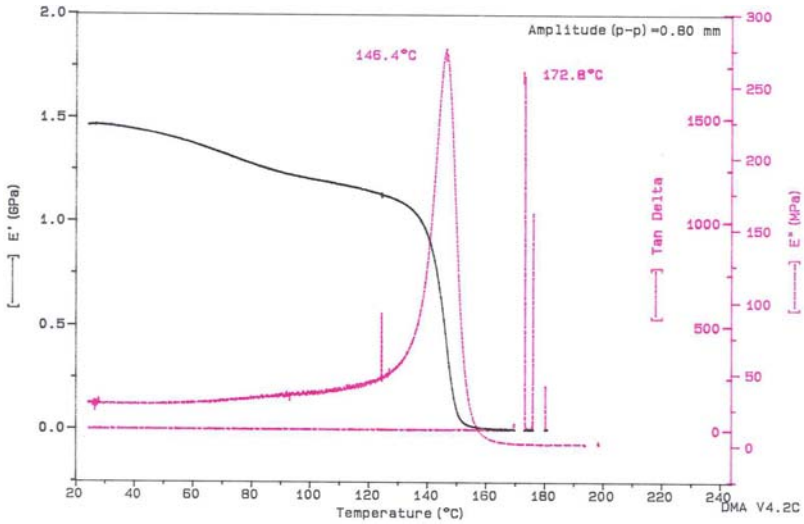

(c)

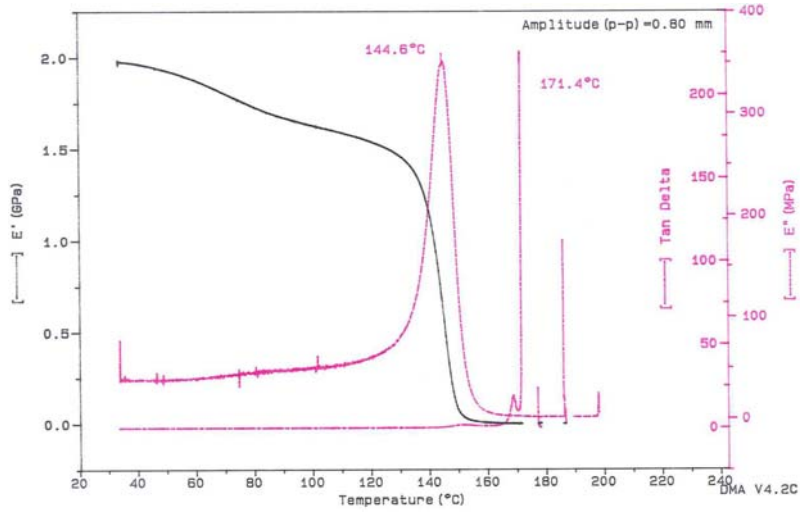

(d)

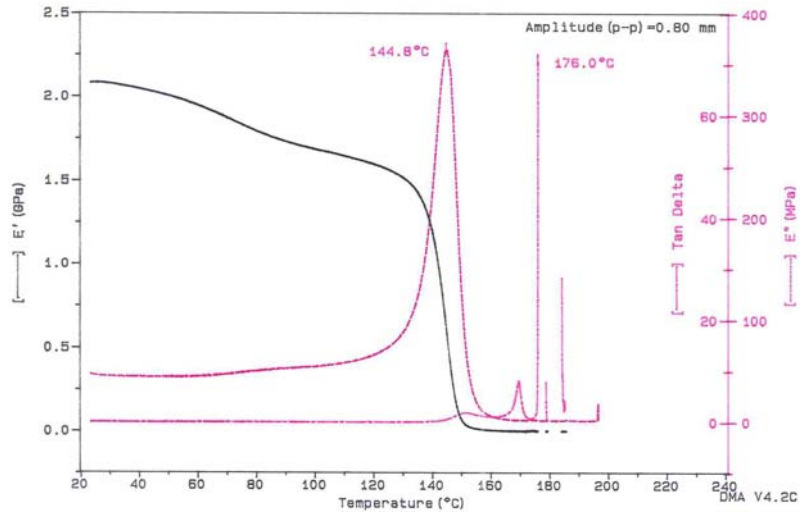

(e)

Figure 3.18 DMA curves of the specimens irradiated up to (a) 0, (b) 20, (c) 44, (d) 96, (e) 136, and (f) 180 kGy (cont'd).

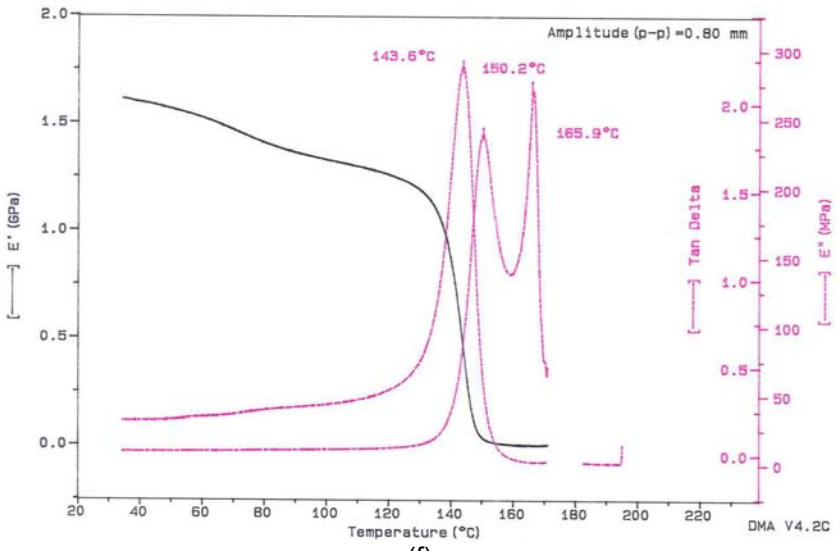

(f)

Figure 3.18 DMA curves of the specimens irradiated up to (a) 0, (b) 20, (c) 44, (d) 96, (e) 136, and (f) 180 kGy (cont'd).

Table 3.11 T_g of the specimens as tanδ peaks

Absorbed Dose (kGy)	T_g (tanδ peaks)
0	170,2
20	174,7
44	172,8
96	171,4
136	176,0
180	165,9

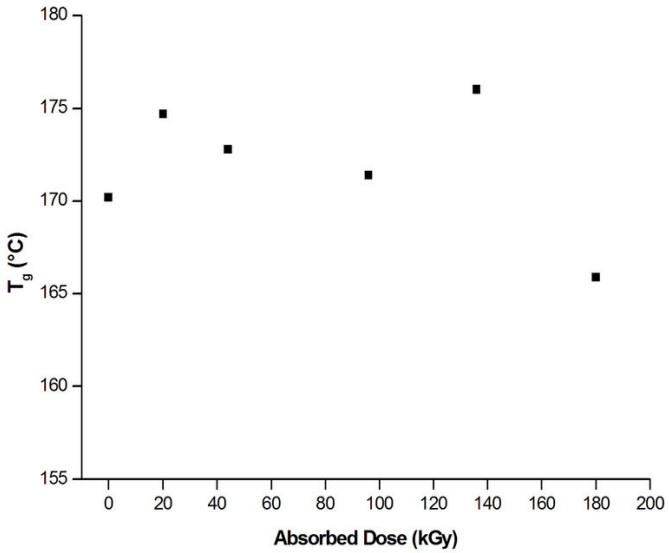

Figure 3.19 Effect of irradiation dose on the T_g (tanδ peaks) of the specimens.

Similar to the trend observed in the values determined by DSC, no steady change is seen on the glass transition temperature versus absorbed dose graph. The T_g of the specimen irradiated up to the maximum dose (180 kGy) is again lower than that of the non-irradiated specimen. It is stated in the literature that the glass transition temperature measured by DMA is slightly higher than that measured by DSC. This is explained by the fact that in a DSC experiment the onset of the transition is usually reported as T_g while in DMA the peak of tanδ gives the center of the relaxation. Additionally, in DMA the frequency effect puts the (mechanically) determined T_g value at a higher point than that determined by DSC [45]. The T_g values determined by DMA in this study (given in Table 3.11) are accordingly higher than those determined by DSC (given in Table 3.10).

3.5.3 Thermogravimetric Analysis

Besides the non-irradiated specimen, 96 and 180 kGy irradiated specimens were subjected to thermogravimetric analysis (TGA) in this study. TGA curves obtained for each specimen are given in Figure 3.20 and Figure 3.21 shows all three curves plotted on the same graph. The TGA curves imply a single-stage degradation at each occasion. The weight loss starts approximately at 400 °C for the non-irradiated specimen, 385 °C for the 96 kGy irradiated specimen and 340 °C for the 180 kGy irradiated specimen. Degradation is maximized at approximately at 540 °C for the non-irradiated specimen, 520 °C for the 96 kGy irradiated specimen, and 510 °C for the 180 kGy irradiated specimen. At 900 °C, the weight losses of the non-irradiated, 96 kGy irradiated and the 180 kGy irradiated specimens were 76% (24% remaining), 77% (23% remaining) and 81% (19% remaining), respectively.

From these results it can be inferred that as the dose increases, the temperature at which degradation starts, as well as the temperature at which the maximum rate of degradation takes place, are slightly decreased. This behavior is in concurrence with the results obtained by Sinha and Dwivedi [29]. Increasing amount of irradiation seems to decrease the thermal stability of the polymer, which may have arisen due to chain scissions in the structure.

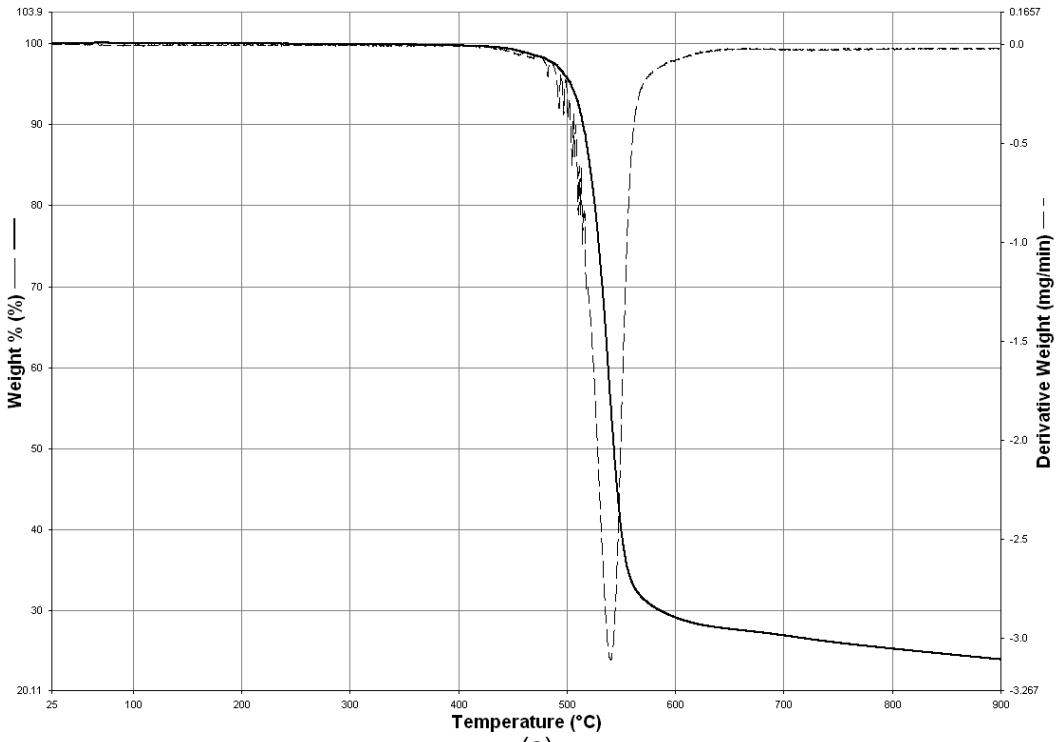

(a)

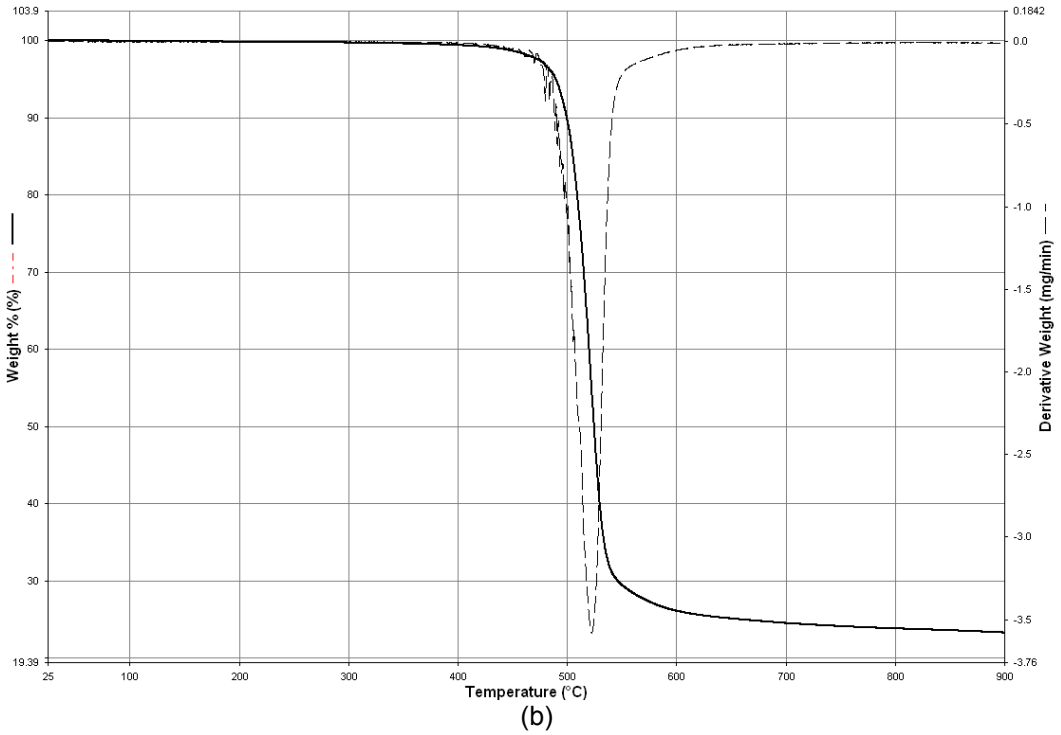

(b)

Figure 3.20 TGA curves of the specimens irradiated up to (a) 0, (b) 96, and (c) 180 kGy.

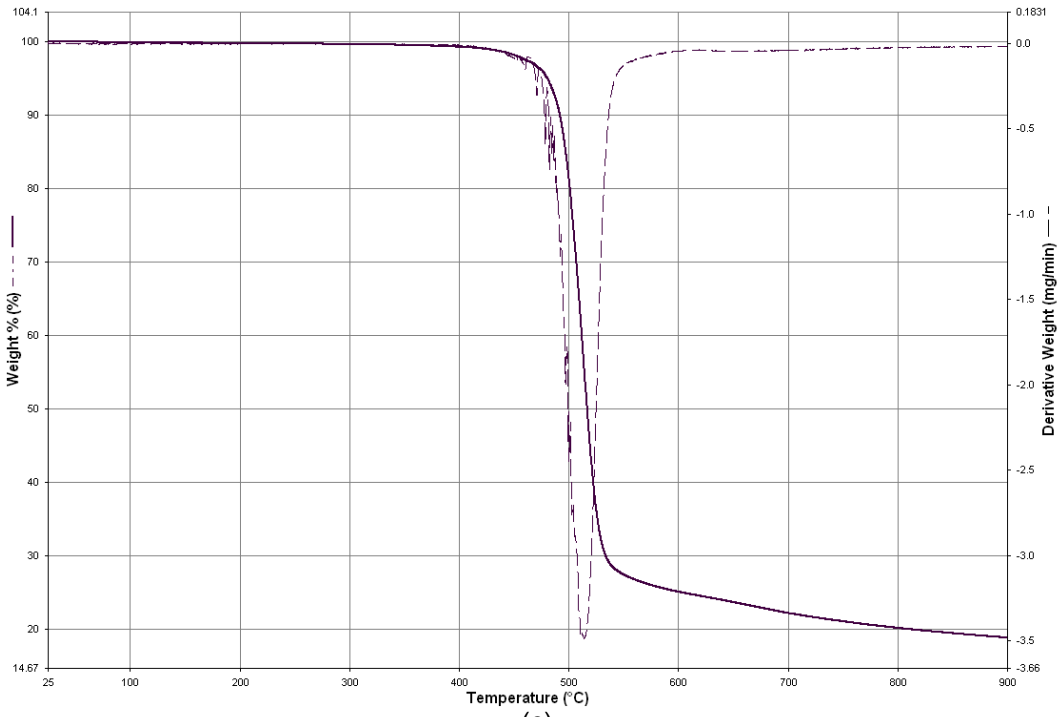

(c)

Figure 3.20 TGA curves of the specimens irradiated up to (a) 0, (b) 96, and (c) 180 kGy (cont'd).

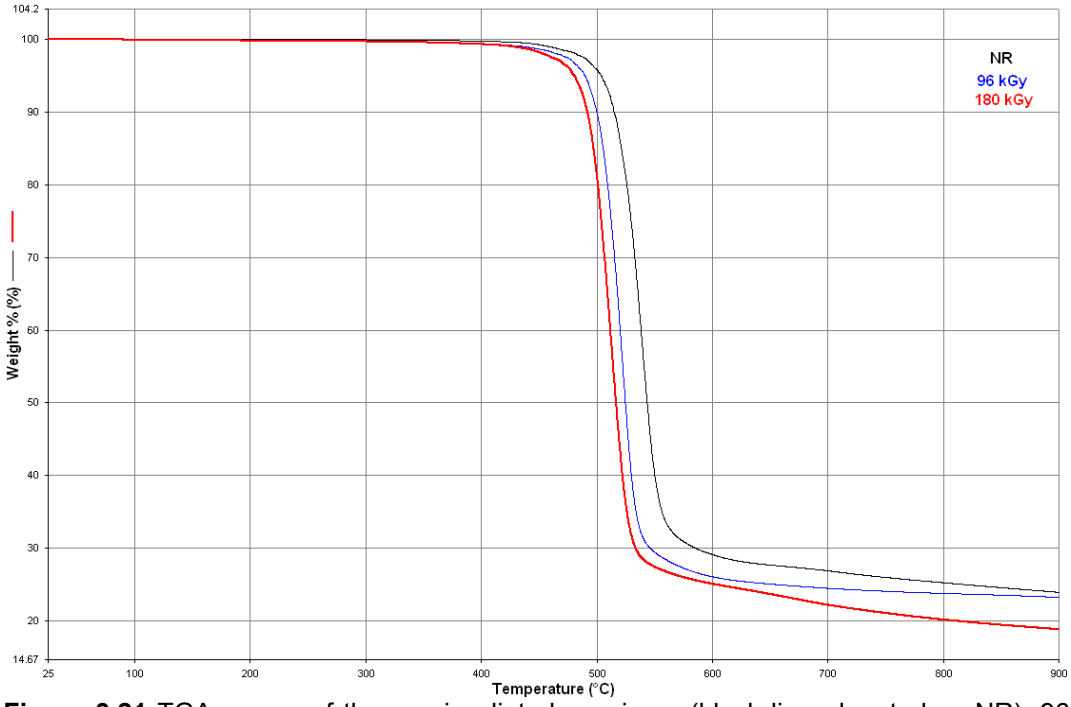

Figure 3.21 TGA curves of the non-irradiated specimen (black line, denoted as NR), 96 kGy irradiated specimen (blue line) and 180 kGy irradiated specimen (red line).

CHAPTER 4

CONCLUSIONS

The following conclusions can be drawn from this study:

1. Upon being subjected to gamma irradiation, the color of polycarbonate turns from transparent to yellow and then to darkening tones of brown as the dose increases.

2. The tensile strength decreases with increasing dose. Chain scissions taking place in the structure under the effect of irradiation is thought to account for this behavior.

3. Irradiating the polymer up to a dose of 180 kGy makes almost no change in the Shore D hardness of the injection molded specimens.

4. The lowest molecular weight values were found to belong to the 96 kGy irradiated specimens. This is also the dose around which average tensile modulus, flexural modulus and flexural strength values exhibit a minimum.

5. The oxidation index decreases as the irradiation dose increases. This could be considered as an indication of carbonyl (C=O) groups being affected by the irradiation, leading to chain scissions.

6. The irradiation scheme applied in this study did not cause a remarkable change in the NMR spectra of polycarbonate.

7. No steady decrease in the glass transition temperature (T_g) of the specimens with increasing dose was observed. The T_g of the specimens irradiated up to the maximum dose (180 kGy), however, were lower than those of the non-irradiated specimens. The T_g values measured by DMA were higher than those measured by DSC.

8. Increasing the amount of absorbed dose results in the beginning and the maximum rate of weight loss to occur at lower temperatures in TGA curves, indicating a decrease in the thermal stability of the polymer presumably due to the greater amount of degradation by irradiation in the structure.

REFERENCES

1. R. L. Clough, “High-Energy Radiation and Polymers: A Review of Commercial Processes and Emerging Applications”, *Nuclear Instruments and Methods in Physics Research B* **185**, 8-33 (2001).

2. T. G. Henry, “Radiation Processing”, *Modern Plastics Encyclopedia*, McGraw-Hill, (1987).

3. “Radiation-Resistant Polymers”, *Concise Encyclopedia of Polymer Science and Engineering*, John Wiley&Sons Inc., (1990).

4. “Polycarbonate”, *Handbook of Plastics, Elastomers & Composites, 4th Edition*, McGraw-Hill, (2002).

5. D. Watson, L. Thomas, “Polycarbonate”, *Modern Plastics Encyclopedia*, McGraw-Hill, (1987).

6. “Polycarbonates”, *Plastics Engineering Handbook, 4th Edition*, Van Nostrand Reinhold Company, (1976).

7. D. G. Powell, “Medical Applications of Polycarbonate”, *Medical Plastics and Biomaterials Magazine*, http://www.devicelink.com/mpb/archive/98/09/003.html, (last visited on 21.01.2009).

8. J. V. Bailey, E. Haag, “Gamma-Radiation Sterilization of Polycarbonate (Meeting Abstract)”, *Plastics Engineering* **39**, 31 (1983).

9. H. W. Bonin, M. W. Walker, V. T. Bui, “Application of Polymers for the Long-Term Storage and Disposal of Low- and Intermediate-Level Radioactive Waste”, *Nuclear Technology* **145**, 82-101, (2004).

10. “Degradation by High Energy Radiation”, *Encyclopedia of Polymer Science and Technology* **6**, Wiley Interscience, 38-41 (2003).

11. “Ionizing radiation”, *Wikipedia, The Free Encyclopedia*, http://en.wikipedia.org/wiki/Ionizing_radiation, (last visited on 19.07.2010).

12. J. H. O’Donnell, D. F. Sangster, *Principles of Radiation Chemistry*, American Elsevier Publishing Company Inc., (1970).

13. D. C. Philips, “Effects of Radiation on Polymers”, *Materials Science and Technology* **4**, 85-91 (1988).

14. G. Hughes, *Radiation Chemistry*, Clarendon Press, (1973).

15. L. A. Pruitt, “The Effects of Radiation on the Structural and Mechanical Properties of Medical Polymers”, *Radiation Effects on Polymers for Biological Use*, Advances in Polymer Science **162**, Springer, (2003).

16. “Gamma ray”, *Wikipedia, The Free Encyclopedia*, http://en.wikipedia.org/wiki/Gamma_ray, (last visited on 19.07.2010).

17. A. Chapiro, “Chemical Modifications in Irradiated Polymers”, *Nuclear Instruments and Methods in Physics Research B* **32**, 111-114 (1988).

18. J. H. Golden, E. A. Hazell, “Degradation of a Polycarbonate by Ionizing Radiation”, *Journal of Polymer Science: Part A* **1**, 1672-1686 (1963).

19. J. H. Golden, B. L. Hammant, E. A. Hazell, “Degradation of Polycarbonates. IV. Effect of Molecular Weight on Flexural Properties”, *Journal of Polymer Science: Part A* **2**, 4787-4794 (1964).

20. A. Torikai, T. Murata, K. Fueki, “Radiation-Induced Degradation of Polycarbonate: Electron Spin Resonance and Molecular Weight Measurements”, *Polymer Degradation and Stability* **7** 55-64 (1984).

21. A. Babanalbandi, D. J. T. Hill, A. K. Whittaker, “An ESR and NMR Study of the Gamma Radiolysis of a Bisphenol-A Based Polycarbonate and a Phthalic Acid Ester”, *Polymers for Advanced Technologies* **9**, 62-74 (1998).

22. E. S. Arajuo, S. M. L. Guedes, “Radiolytic Degradation and Stability of Polycarbonate”, *Polymer Preprints (USA)* **34**, 205-206 (1993).

23. D. Acierno, F. P. La Mantia, G. Titomanli, E. Calderaro, F. Castiglia, “γ-Radiation Effects on a Polycarbonate”, *Radiation Physics and Chemistry* **16**, 95-99 (1980).

24. A. K. Kalkar, S. Kundagol, S. Chand, S. Chandra, “Effect of Gamma-Irradiation on Structural and Electrical Properties of Poly(Bisphenol-A Carbonate) Films”, *International Journal of Radiation Applications and Instrumentation. Part C. Radiation Physics and Chemistry* **39**, 435-442 (1992).

25. E. S. Arajuo, H. J. Khoury, S. V. Silveira, “Effects of Gamma-Irradiation on Some Properties of Durolon Polycarbonate”, *Radiation Physics and Chemistry* **53**, 79-84 (1998).

26. J. V. Bailey, L. Haag, *Gamma Radiation Sterilization of Polycarbonate*, Mobay Chemical Corporation, Pittsburgh, (1983).

27. N. S. de Melo, R. P. Weber, J. C. M. Suarez, "Toughness Behavior of Gamma-Irradiated Polycarbonate", *Polymer Testing* **26** 315-322 (2007).

28. D. Sinha, K. L. Sahoo, U. B. Sinha, T. Swu, A. Chemseddine, D. Fink, "Gamma-Induced Modifications of Polycarbonate Polymer", *Radiation Effects & Defects in Solids* **159**, 587-595 (2004).

29. D. Sinha, K. K. Dwivedi, "Radiation-Induced Modification on Thermal Properties of Different Nuclear Track Detectors", *Radiation Measurements* **36**, 713-718 (2003).

30. T. Özdemir, A. Usanmaz, "Degradation of Poly(carbonate urethane) by Gamma Irradiation", *Radiation Physics and Chemistry* **76**, 1069-1074 (2007).

31. T. Özdemir, A. Usanmaz, "Degradation of Poly(bisphenol-a-epichlorohydrin) by Gamma Irradiation", *Radiation Physics and Chemistry* **77**, 799-805 (2008).

32. T. Özdemir, A. Usanmaz, "Use of Poly(methyl methacrylate) in Radioactive Waste Management: I. Radiation Stability and Degradation", *Progress in Nuclear Energy* **51**, 240-245 (2009).

33. E. Vargün, A. Usanmaz, "Degradation of Poly(2-hydroxyethyl methacrylate) Obtained by Radiation in Aqueous Solution", *Journal of Macromolecular Science, Part A*, **47**, 882-891 (2010).

34. F. Hacıoğlu, "Degradation of EPDM via Gamma Irradiation and Possible Use of EPDM in Radioactive Waste Management", M. S. Thesis, METU (2010).

35. Plastics - Determination of tensile properties - Part 1: General Principles, International Standard, ISO 527-1:1993(E).

36. Plastics - Determination of flexural properties, International Standard, ISO 178:1993(E).

37. M. Chanda, S. K. Roy, *Plastics Fundamentals, Properties and Testing*, CRC Press, (2009).

38. *Handbook of Polymer Testing*, Rapra Technology Limited, (2002).

39. P. J. Flory, *Principles of Polymer Chemistry*, Cornell University Press, (1953).

40. F. W. Billmeyer, *Textbook of Polymer Science, 3rd Edition*, John Wiley&Sons, (1984).

41. R. J. Young, P. A. Lowell, *Introduction to Polymers, 2nd Edition*, Chapman & Hall, (1991).

42. J. R. Fried, *Polymer Science & Technology, 2nd Edition*, Prentice Hall PTR, (2003).

43. "Gel permeation chromatography", *Wikipedia, The Free Encyclopedia*, http://en.wikipedia.org/wiki/Gel_permeation_chromatography, (last visited on 18.06.2010).

44. B. H. Stuart, *Polymer Analysis*, John Wiley & Sons Ltd., (2002).

45. N. P. Cheremisinoff, *Polymer Characterization*, Noyes Publications, (1996).

46. "Differential scanning calorimetry", *Wikipedia, The Free Encyclopedia*, http://en.wikipedia.org/wiki/Differential_scanning_calorimetry, (last visited on 18.06.2010).

47. "Dynamic mechanical analysis", *Wikipedia, The Free Encyclopedia*, http://en.wikipedia.org/wiki/Dynamic_mechanical_analysis, (last visited on 18.06.2010).

48. *Polymer Handbook, 4th Edition*, John Wiley&Sons, (1999).